Marine and Petroleum Geology 147 (2023) 105975

Contents lists available at ScienceDirect

Marine and Petroleum Geology

journal homepage: www.elsevier.com/locate/marpetgeo

Late Quaternary sedimentary record of estuarine incised-valley filling and interfluve flooding: The Manfredonia paleovalley system (southern Italy)

Alessandro Amorosi [a,*], Luigi Bruno [b], Massimo Caldara [c], Bruno Campo [a], Simone Cau [a], Vincenzo De Santis [c], Andrea Di Martino [a], Wan Hong [d], Giorgio Lucci [a], Claudio Pellegrini [e], Veronica Rossi [a], Irene Sammartino [e], Stefano Claudio Vaiani [a]

[a] Department of Biological, Geological and Environmental Sciences (BiGeA), University of Bologna. Piazza di Porta San Donato 1, 40126, Bologna, Italy
[b] Department of Chemical and Geological Sciences, University of Modena and Reggio Emilia, Via Campi 103, 41125, Modena, Italy
[c] Department of Earth and Geonvironmental Sciences, University of Bari "Aldo Moro", Via Orabona 4, 70125, Bari, Italy
[d] KIGAM Korea Institute of Geoscience and Mineral Resources, 92 Gwahangro, Yuseong-gu, Daejeon Metropolitan City, South Korea
[e] National Research Council (CNR), Institute of Marine Science (ISMAR), Via Gobetti 101, 40129, Italy

ARTICLE INFO

Keywords:
Sequence stratigraphy
Source-to-sink
Incised valley
Mollusk
Meiofauna
Geochemistry
Apulia
Adriatic sea

ABSTRACT

Multiple paleovalley systems of late Quaternary age have been widely explored in previous research from the Gulf of Manfredonia on the basis of seismic data, but only limited information is available on their proximal (onshore) segments. Through an integration of sedimentary, paleoecological (mollusks, benthic foraminifers, ostracods), and geochemical analyses from three 30-50 m-long onshore cores and a sequence-stratigraphic framework chronologically constrained by 25 radiocarbon data, we document the stratigraphic architecture of three contiguous paleovalley systems (Candelaro, Cervaro and Carapelle rivers) and their sedimentary response to Late Pleistocene valley excavation, Holocene filling and basinwide interfluve flooding. Above a prominent sequence boundary formed during the Late Pleistocene relative sea-level fall, fluvial-channel gravels and sands (lowstand systems tract) are overlain by a deepening-upward, valley-fill succession of inner-estuarine (freshwater) to outer-estuarine (brackish) muds (lower transgressive systems tract – TST). The individual valley fills are overlain by laterally extensive bay deposits (upper TST) and by a progradational succession of prodelta/delta front and offshore/shoreface deposits that reflect normal regression under highstand conditions (HST). The transition from fluvial to inner-estuary (fluvial-dominated) and outer-estuary (wave-influenced) deposits records the progressive shift in sediment provenance from Southern Apennine source rocks to a mixed composition that reflects increasing alongshore sediment contribution from northern sources via the SE-directed Western Adriatic Current. The stratigraphic surface that demarcates the transition from estuarine to bay depositional systems (lower/upper TST boundary) represents the physical prolongation of interfluvial terrace surfaces, as valley margins were flooded during the Early Holocene transgression. This surface, typically recognizable on seismic profiles at the boundary between low-amplitude and overlying high-amplitude reflectors, has no obvious lithologic signature in core. However, it can be readily identified on the basis of paleoecologic features (sharp increase in species diversity and in the proportion of marine taxa) that reveal the abrupt transition from laterally confined to unconfined settings.

1. Introduction

Incised valleys (Van Wagoner et al., 1990) or paleovalley systems (Blum and Törnqvist, 2000) are important features in the stratigraphic record: they represent fluvially-eroded, elongate topographic lows that are typically larger than single channel forms (Zaitlin et al., 1994; Boyd et al., 2006; Gibling et al., 2011). Beneath low-gradient Holocene coastal plains, paleovalleys typically display significant relief, with truncation of older strata and juxtaposition of fluvial/estuarine facies onto marine deposits (Van Wagoner et al., 1990; Blum et al., 2013).

Paleovalley systems develop during phases of base-level lowering, and their fill is associated with relative sea-level rise (Posamentier and

* Corresponding author.
E-mail address: alessandro.amorosi@unibo.it (A. Amorosi).

https://doi.org/10.1016/j.marpetgeo.2022.105975
Received 8 August 2022; Received in revised form 9 October 2022; Accepted 10 October 2022
Available online 21 October 2022

Vail, 1988; Posamentier et al., 1988; Wright and Marriott, 1993). Examples from Quaternary across-shelf paleovalleys (Thomas and Anderson, 1994; Abdulah et al., 2004) have documented that the post-MIS 5e glacial-interglacial cycle, spanning approximately the last 125 kyr, includes multiple periods of incision punctuated by episodes of lateral migration, valley widening, and channel-belt deposition during relative sea-level fall, resulting in the formation of compound incised valleys (Blum and Törnqvist, 2000; Rittenour et al., 2005; Busschers et al., 2007; Labaune et al., 2010; Blum et al., 2013; Mattheus et al., 2020).

Criteria for identifying paleovalley fills in the geological record have commonly been derived from coastal areas, where high-magnitude glacio-eustatic fluctuations generate predictable systems tracts (Boyd et al., 2006; Gibling et al., 2011). Paleovalleys buried at shallow depths beneath modern coastal plains are inferred to have formed during the most recent relative sea-level fall, at the MIS 3-2 transition (Blum and Price, 1998; Dabrio et al., 2000; Li et al., 2000; Autin and Aslan, 2001; Anderson et al., 2004; Busschers et al., 2007; Kasse et al., 2010; Amorosi et al., 2013; Fan et al., 2019). For such coastal-plain paleovalleys, the rate and magnitude of relative sea-level change is the primary control on stratigraphic organization (Wang et al., 2020) and paleovalley fills typically include estuarine successions formed during shoreline transgression (Dalrymple et al., 1994; Zaitlin et al., 1994; Boyd et al., 2006; Dalrymple, 2006; Blum et al., 2013).

Few paleovalley systems have been reported from offshore locations along the southern Adriatic coast of Italy. A deeply incised valley (the "Manfredonia incised valley" – MIV in Fig. 1) was first documented from the Gulf of Manfredonia, south of the Gargano Promontory, on the basis of seismic profiles interpretation (Maselli and Trincardi, 2013; Maselli et al., 2014). Three distinct paleovalley systems, deeply incised (40 m) in the substrate, were then identified off Apulia in a more southern position, about 80 km from the shelf edge (De Santis and Caldara, 2016; De Santis et al., 2020a, b). While Quaternary incised valleys have been abundantly investigated along the Apulian shelf, little work has addressed the geometry and facies architecture of the onshore segments of the valleys (Amorosi et al., 2016).

This study relies on the integrated sedimentological, paleontological (mollusk, benthic foraminifer and ostracod) and geochemical analysis of a 50 m-long core (MAN) that was recovered in onshore position in May 2021, in front of the Manfredonia incised valley (Fig. 1). It is also based on insights from cores ZS1 and ZS2 recovered 15 km south of Core MAN, and from a 17 km-long transect with detailed geochronology of 25 radiocarbon ages (Fig. 1). For a preliminary description of core ZS2, the reader is referred to De Santis et al. (2020a).

2. Geological setting

The Tavoliere plain, in Apulia, is the second largest alluvial plain in Italy and represents the onshore prolongation of the Manfredonia Gulf (Fig. 1). It is drained by three short rivers, from north to south: Candelaro (70 km), Cervaro (30 km), and Carapelle (85 km). The longer Ofanto River (165 km) also flows into the southern part of the Manfredonia Gulf (Fig. 1). The Tavoliere plain belongs to the Bradanic Trough domain, which formed in the Early Pliocene, between the Southern Apennine chain and the Apulian–Dinaric foreland (Malinverno and Ryan, 1986; Royden et al., 1987; Patacca and Scandone, 1989, 2001; Doglioni, 1991). A generalized regional uplift took place in the area from the Middle Pleistocene (Ricchetti et al., 1992; Doglioni et al., 1994, 1996), as testified by a well exposed series of uplifted terrace deposits cropping out extensively along the Tavoliere (De Santis et al., 2010, 2013, 2014) and in other parts of Apulia (De Santis et al., 2020c).

Glacio-eustatic fluctuations superposed on this ongoing phase of regional uplift punctuated the overall regressive trend. As a consequence, terrace deposits of the Apulian Tavoliere record a complex pattern of alternating Pleistocene marine and continental deposits (Caldara and Pennetta, 1991, 1993; Boenzi et al., 1991; Apulian Tavoliere Supersynthem of Ciaranfi et al., 2011).

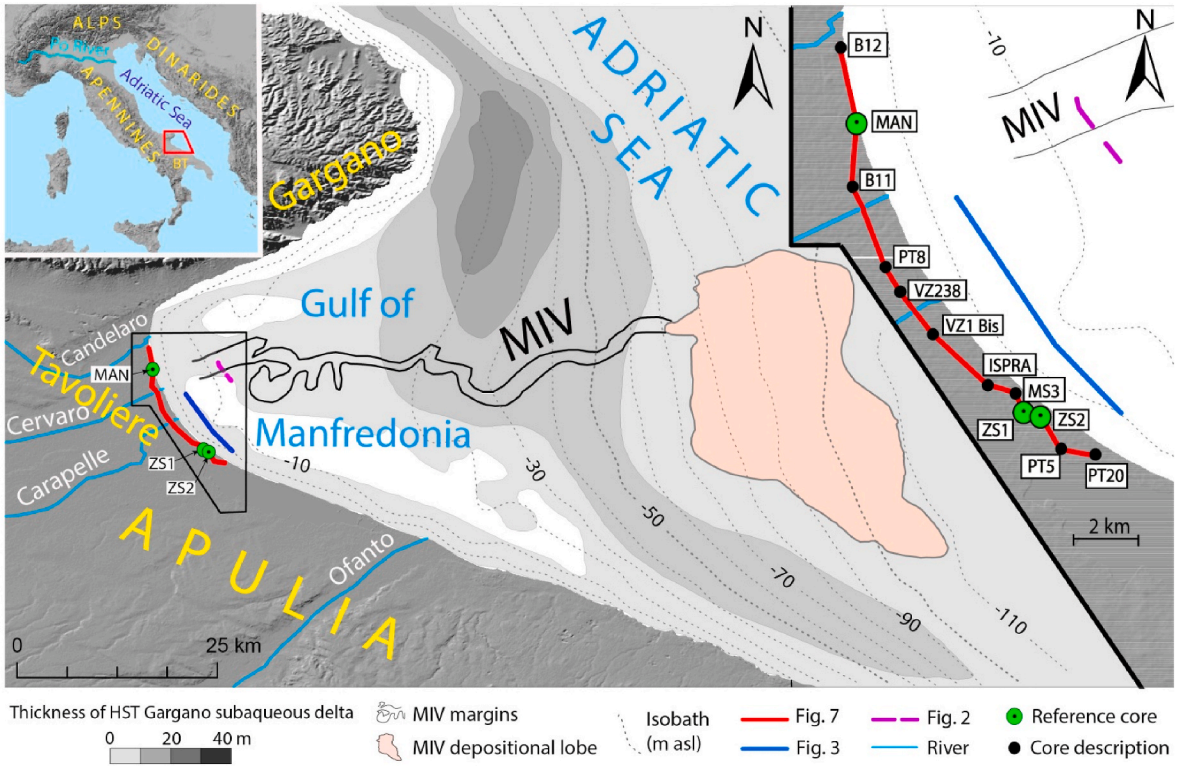

Fig. 1. Simplified bathymetric map of the Gulf of Manfredonia, with location of reference cores MAN, ZS1 and ZS2, offshore seismic profiles (Figs. 2 and 3) and the onshore stratigraphic panel (Fig. 7). The Manfredonia paleovalley (MIV), the contour of present-day bathymetry (after Maselli et al., 2014), and the Gargano subaqueos delta of Cattaneo et al. (2003) are also shown. BT: Bradanic trough.

Apulian river catchments around the Gulf of Manfredonia comprise sedimentary rocks exposed in the Gargano Promontory and in the Southern Apennines. Mesozoic carbonates of the Apulia platform crop out in the Gargano massif, whereas silty clay hemipelagic deposits are the dominant lithology of the Bradanic Trough, which was supplied mostly from the southern Apennines (Ricchetti et al., 1992).

The Gulf of Manfredonia has a microtidal regime and a very gently sloping sea bottom toward the east. Distinct cross-shelf paleovalley systems related to the Last Glacial Maximum (LGM) have been described in detail from this region (Fig. 1). The Manfredonia incised valley, fed by Candelaro River, was described first by Maselli and Trincardi (2013), who identified a sinuous valley elongated for more than 60 km in W-E direction, from the inner to the outer shelf, with its prolongation into a depositional lobe, at 80–100 m depth (Fig. 1). Based on seismic surveys with sub-bottom profiler, the same valley was intercepted at relatively proximal locations by De Santis and Caldara (2016 - Fig. 2). More recently, two adjacent incised-valley systems, one linked to the Cervaro River, and the other one generated by incision of the Carapelle River (Fig. 1), have been illustrated by De Santis et al. (2020b).

A regionally extensive stratigraphic surface represents the lowstand surface of subaerial exposure formed during the LGM (Maselli and Trincardi, 2013; Maselli et al., 2014). This surface separates a poorly reflective unit, of pre-LGM age, from overlying, reflective units of latest Pleistocene to Holocene age that represent the lowstand/transgressive systems tracts and exhibit distinctive onlapping geometries (De Santis and Caldara, 2016 – Fig. 2).

Above a regional downlap surface that marks the maximum flooding surface, highstand deposits in the study area include progradation of the mud-prone Gargano subaqueous delta (Cattaneo et al., 2003; Pellegrini et al., 2015), which represents the southernmost portion of the Western Adriatic mud wedge (Fig. 1).

3. Methods

This study is based primarily on the sedimentological analysis of undisturbed core material from three reference cores (Fig. 1): core MAN (41°32′55.528"N, 15°53′53.417"E), core ZS1 (41°27′22.008"N, 15°57′15.233"E), and core ZS2 (41°27′16.869"N, 15°57′35.449"E). For the stratigraphic analysis of the study succession, we also used archived borehole descriptions and data from earlier work (De Santis and Caldara, 2016; De Santis et al., 2020a, b, c). Reference cores were investigated through combined sedimentologic and paleontologic investigations. Sedimentary facies analysis of the study cores was carried out through description of lithology, grain size, primary sedimentary structures, lamination styles, accessory components and resistance to penetration measured through a pocket penetrometer. Mollusks, benthic foraminifers and ostracods were analyzed to detect changes in depth, salinity, degree of confinement, type of substrate, oxygen and food availability (Scarponi and Kowalewski, 2004; Rossi and Vaiani, 2008; Amorosi et al., 2014; Scarponi et al., 2014; Wittmer et al., 2014; Mazzini et al., 2017, 2022). Comparison with spatial distribution patterns of the modern meiofauna and mollusks allowed a robust environmental interpretation of fossil assemblages (Scarponi et al., 2022).

Core samples for macrobenthic analysis, ~250 cm^3 each, were collected at ~1 m intervals. Samples were dried (24 h at 40 °C), soaked in 4% H_2O_2 solution (~12 h), and wet sieved with 1 mm screen (Scarponi and Angeletti, 2008). The resulting material was qualitatively analyzed under an optical microscope to recognize environmental key taxa in each fossil assemblage. Macrobenthic remains of key taxa were counted as rare ($n \leq 10$) or common ($n > 10$ fossils) and identified, whenever possible, to species level.

A total of 136 samples, ~100 g of dry weight each, were collected for analysis of foraminiferal and ostracod assemblages (60 from core MAN; 41 from core ZS1; 35 from core ZS2). Samples treatment followed the standard method adopted in several studies from the Adriatic coastal plain (Rossi and Vaiani, 2008; Barbieri et al., 2017). Sediment samples were: (i) dried for 8 h at 60 °C, (ii) soaked in water, (iii) wet sieved through sieves of 63 μm (240 mesh), (iv) dried again for at least 8 h and weighted, and (v) dry sieved at 125 μm. Size fractions >125 μm and 63–125 μm were analyzed separately.

Species identification was based upon: (i) original descriptions (Supplementary Table 1 – Ellis and Messina, 1940, 1952), (ii) reference papers that were also used for paleoenvironmental interpretations (Athersuch et al., 1989; Cimerman and Langer, 1991; Henderson, 1990; Jorissen, 1988; Mazzini et al., 2022; Milker and Schmiedl, 2012; Sgarrella and Moncharmont Zei, 1993), and (iii) additional studies (Debenay et al., 2000; De Stigter et al., 1998; Frezza and Carboni, 2009; Jorissen et al., 2018; Murray, 2006; Salel et al., 2016). For the complete taxonomic reference list, see Supplementary Table 1.

The geochemical characterization of Southern Apennines sediment sources was carried out through analysis of 11 Apulian river samples collected from Candelaro (3 samples), Cervaro (3), Carapelle (2) and Ofanto (3). Samples were retrieved from exposed bars or subaqueous channel beds, and all particle sizes, from coarse sand to mud, were considered. Thirty-three samples from core MAN (between 43.10 and 8.70 m depth) were also analyzed for bulk-sediment geochemistry. Samples were analyzed at Bologna University laboratories for major element oxides, the loss on ignition (LOI) and trace elements. LOI, evaluated after overnight heating at 950 °C (LOI_{950}), represents a measure of volatile substances (weight %, wt%), including pore water, inorganic carbon and organic matter. The estimated precision and accuracy for trace-element determinations was 5%, except for elements with concentrations <10 ppm, for which the accuracy was 10%.

A total of 25 radiocarbon dates (12 from core MAN, 1 from core

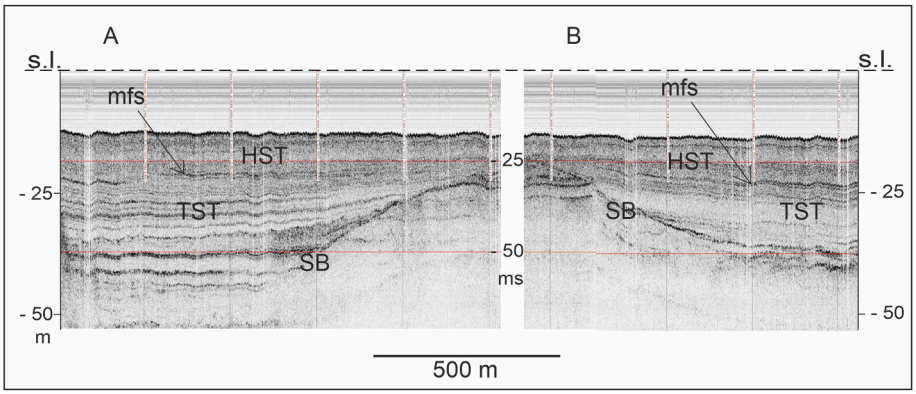

Fig. 2. Seismic profile showing the Manfredonia paleovalley (left) and the adjacent Cervaro River paleovalley (right), both cut into the Quaternary substrate, and their sequence-stratigraphic interpretation (SB: sequence boundary, TST: transgressive systems tract, HST: highstand systems tract, mfs: maximum flooding surface). Slightly modified from De Santis and Caldara (2016). For section trace, see Fig. 1.

VZ238, 4 from core ZS1 and 8 from core ZS2), including a graded, light grey pumice layer (Mercato Pumice in De Santis et al., 2020b) were carried out mostly at KIGAM laboratories, Daejeon City, Korea (Table 1). The calibration of conventional radiocarbon ages was based on the IntCal20 dataset (Reimer et al., 2020), using OxCal 4.3. (Bronk Ramsey, 2009). Before AMS counting, organic samples (for example, wood) were pre-treated with acid–alkali–acid method in order to remove $CaCO_3$ and humic-acids contamination. Shell samples were subjected to HCl etches to eliminate secondary carbonate component. Peat samples were treated with 0.5M NaOH at 80 °C for 2 h to extract humic acid without extraction of the humin fraction. Humic acids were then collected by adding concentrated hydrochloric acid to the solution. Results are summarized in Table 1.

With the aim of building a model for routing of sediment across all segments of the Apulian source-to-sink system, we also reinterpreted the seismic profile by De Santis et al. (2020b), located about 2.5 km seaward of the study cores (Fig. 1), which allowed us to carry out onshore-to-offshore stratigraphic correlation.

4. Offshore seismic stratigraphy

The stratigraphic architecture of two adjacent incised-valley systems, generated by incision of the Cervaro and Carapelle rivers, respectively, has been illustrated in detail by De Santis et al. (2020a), who identified four seismic units with clear sequence-stratigraphic significance. In this study, we expand upon previous work by differentiating two additional seismic units that characterize the post-LGM succession in the study area (Fig. 3). Seismic units 1–3 are laterally confined by the pre-LGM substrate and represent the paleovalley fill, whereas units 4–6 are laterally extensive and overlie the adjacent interfluves. The six seismic units that form the LGM/post-LGM sedimentary succession are illustrated in stratigraphic order (Fig. 3).

4.1. Seismic Unit 1

This unit has onlapping geometry onto the sequence bounding unconformity, though the lack of coherent reflections obscures individual onlap reflection terminations onto the erosional depression. Unit 1 is characterised by low-amplitude, spaced, sub-horizontal to slightly wavy reflections, of low lateral continuity (Fig. 3). Overall, it is characterised by chaotic fill internal reflection configuration (Fig. 3).

The chaotic fill reflection configuration of Unit 1 suggests the presence of poorly stratified sediment bodies filling the lower parts of paleovalleys, deposited in a relatively high-energy setting (Sangree and Widmier, 1977). Earlier documentations sustain interpretation of this unit as a fluvial deposit (Maselli and Trincardi, 2013).

4.2. Seismic Unit 2

This unit is onlapping onto the sequence bounding unconformity. It consists predominantly of low-amplitude and low-continuity seismic reflections, with locally higher-amplitude reflections with sub-horizontal configuration (Fig. 3). Along the valley axis, Unit 2 shows meter-scale, channel-like incisions highlighted by high-amplitude reflections with scarce lateral continuity (Fig. 3).

Unit 2 is interpreted as a silt/mud facies affecting a broad section of the valley, which represents further valley filling in a locally high-energy depositional environment (Mitchum et al., 1977), as testified by the association with local cut-and-fill events.

4.3. Seismic Unit 3

This unit, <5 m thick, is characterised by closely-spaced, discontinuous, parallel to sub-parallel reflections, with low-to high-amplitude. Locally, laterally continuous, very high-amplitude reflections lap onto the paleovalley flanks (Fig. 3). This unit shows internal onlap and downlap reflection terminations (Fig. 3).

Unit 3 represents the topmost part of the paleovalley fill. Its internal reflection configuration suggests multiple depositional events that resulted in compensational stacking patterns. These events led to deposition of stratified sedimentary bodies of variable grain size, as suggested by changes in seismic amplitude calibrated by sediment cores in the same area (Maselli and Trincardi, 2013).

4.4. Seismic Unit 4

This unit consists of discontinuous, low-amplitude reflectors overlapping the interfluves and discontinuous, low-to high-amplitude reflectors above the valley fill (Fig. 3). On the paleovalley flanks, Unit 4 reaches a maximum thickness of 5 m. The topmost reflector of this unit

Table 1
List of radiocarbon dates in Figs. 4 and 7.

Lab code	Sample name and depth (m)	Material	conventional 14C age (year BP)	d13C (‰)	calibrated 14C age (year BP)
KGM-OCa210086	MAN 4,1	shell	786 ± 31	−4.4 ± 1.7	240 ± 160
KGM-OCa210088	MAN 9,75	shell	1264 ± 30	6.69 ± 1.45	655 ± 120
KGM-OCa210089	MAN 13,7	shell	1488 ± 32	0.78 ± 1.43	865 ± 140
KGM-OCa210090	MAN 20,27	shell	6479 ± 42	−1.64 ± 2.3	6240 ± 210
KGM-OCa210091	MAN 21,8	shell	6522 ± 42	−0.95 ± 2.63	6285 ± 210
KGM-OCa210092	MAN 23,45	shell	6708 ± 44	−0.96 ± 2.42	6485 ± 220
KGM-OCa210093	MAN 24,8	shell	6986 ± 43	−1.25 ± 1.53	6800 ± 230
KGM-OCa210094	MAN 25,8	shell	8376 ± 45	0.59 ± 1.09	8200 ± 200
KGM-OCa210096	MAN 27,83	shell	8554 ± 46	−3.79 ± 1.41	8390 ± 220
KGM-OCa210097	MAN 28,45	shell	8841 ± 47	−4.69 ± 1.26	9380 ± 140
KGM-OWd210410	MAN 30,9	wood	8722 ± 44	−31.03 ± 0.92	9690 ± 200
KGM-OWd210411	MAN 31,2	wood	8819 ± 40	−25.92 ± 1.95	9890 ± 260
KGM-OCa210076	ZS1 3,4	shell	2488 ± 33	1.24 ± 1.73	1425 ± 90
KGM-OCa210077	ZS1 19,75	shell	4633 ± 36	0.96 ± 2	4055 ± 240
KGM-OCa210078	ZS1 24,38	shell	8357 ± 45	−3.34 ± 2.22	8735 ± 210
KGM-OCa210079	ZS1 25,55	shell	8021 ± 44	−2.65 ± 1.28	8345 ± 120
D-AMS 007669	ZS2 4,8	shell	2090 ± 23	5.8 ±	1020 ± 95
KGM-OCa210080	ZS2 12,3	shell	2801 ± 34	−2.2 ± 1.24	1780 ± 220
KGM-OCa210081	ZS2 14,1	shell	2874 ± 35	0.01 ± 1.24	1870 ± 210
KGM-OCa210082	ZS2 16,3	shell	4369 ± 37	7.12 ± 2.15	3705 ± 230
KGM-OCa210083	ZS2 19,1	shell	4309 ± 37	3.32 ± 0.99	3630 ± 230
KGM-OCa210084	ZS2 27,7	shell	8398 ± 51	1.31 ± 3.15	8800 ± 210
D-AMS 007669	ZS2 28,65	wood	8401 ± 37	−14.3 ±	9160 ± 163
KGM-OSa210085	ZS2 29,95	sediment	8418 ± 39	−20.87 ± 1.69	9450 ± 100
KGM-OCa210085	VZ238 4	shell	6576 ± 43	0.83 ± 0.71	6350 ± 210

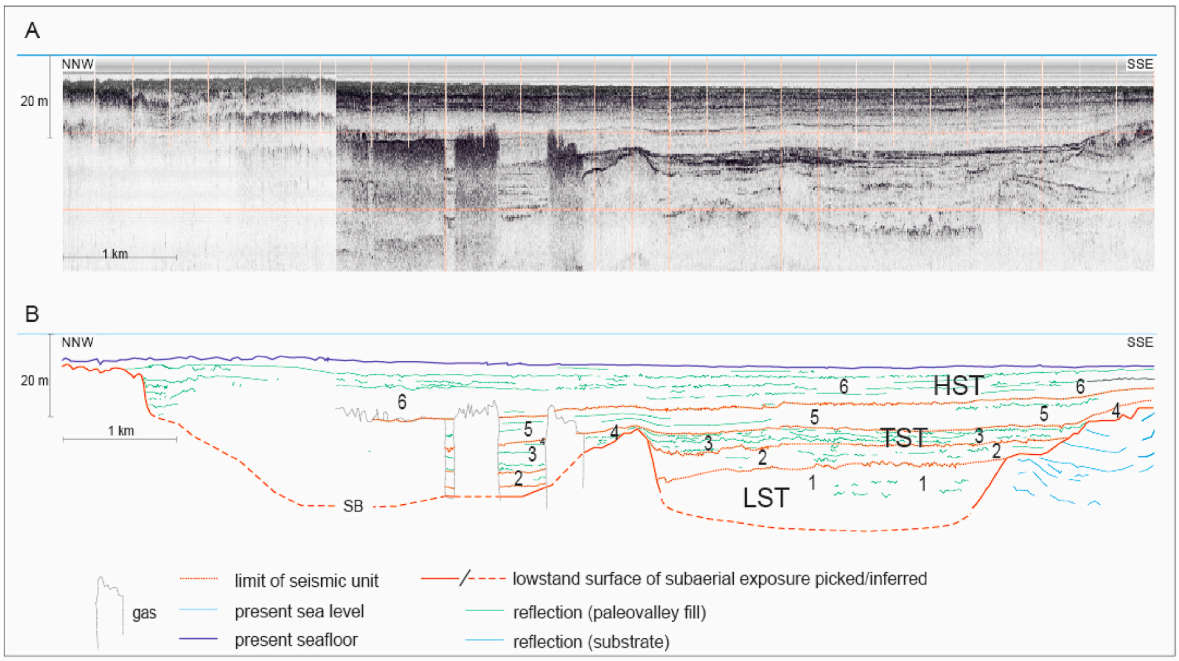

Fig. 3. Seismic profile (A) across the Cervaro (left) and Carapelle (right) paleovalleys, with subdivision of the LGM (Unit 1) and post-LGM (Units 2–6) sedimentary succession into six seismic units (B) and their sequence-stratigraphic interpretation (LST: lowstand systems tract, TST: transgressive systems tract, HST: highstand systems tract). Modified after De Santis et al. (2020a). Facies architecture is shown in Fig. 7. For section trace, see Fig. 1. SB: sequence boundary.

dips toward the valley axis (Fig. 3).

The seismic reflection configuration of Unit 4 and its lateral changes in thickness and inclination suggest progradation of coarse-grained lithosomes above the southeastern paleovalley flank. The prograding sediment body suggests increasing accommodation compared to earlier phases of valley filling. In this context, the rollover point (i.e. the main breaking in slope) of the coarse-grained lithosome approximates the coastline position and suggests a very shallow-water environment, with local (bay-head delta?) progradation (Pellegrini et al., 2020).

4.5. Seismic Unit 5

This unit has low amplitude reflections, with only few, widely-spaced, parallel and slightly dipping high-amplitude reflections of high lateral continuity (Fig. 3). These reflections have slightly wavy geometry above the interfluves. Overall, Unit 5 shows prograding reflection patterns (Fig. 3).

The seismic pattern of Unit 5 suggests deposition of fine-grained clinoforms in a lower-energy (deeper) environment compared to underlying seismic units. Muddy clinoforms prograding from the north and along the Adriatic coast show a depocenter in the Gulf of Manfredonia and extend further south (e.g. Cattaneo et al., 2003; Pellegrini et al., 2015), being intersected along the seismic profile in Fig. 3.

4.6. Seismic Unit 6

This unit is characterised by closely-spaced, gently dipping reflections, with moderate to high amplitude and high lateral continuity. Locally, toplap and offlap terminations are present (Fig. 3). Unit 6 shows an overall prograding fill configuration (Fig. 3).

Unit 6 seismic configuration suggest the presence of stacked fine-grained prograding clinoforms with compensational stacking patterns (Mitchum et al., 1977). Similar prograding clinoforms have been documented from the central Adriatic Sea as the result of the interplay among sediment supply, accommodation, and oceanographic regime (Pellegrini et al., 2021).

5. Onshore sedimentary facies associations

Six facies associations were differentiated through the integration of sedimentological and paleoecological data from reference cores MAN, ZS1, and ZS2 (Fig. 4). These facies associations are illustrated below, in stratigraphic order. Unless specified otherwise, data refer to core MAN.

5.1. Fluvial-channel facies association

5.1.1. Description

This facies association, up to 10 m thick, but only partly recovered in core MAN (Fig. 4), was reconstructed using stratigraphic descriptions from adjacent continuously-cored boreholes (De Santis et al., 2010, 2013). It consists of laterally amalgamated, gravel and coarse to medium sand bodies that grade upwards into fine to silty sand and sand-silt alternations (Fig. 4). Gravel and sand bodies have concave-up, lens-shaped geometry, erosional lower boundaries and are locally separated by thin clay horizons. Gravels, of Apennine origin, are poorly sorted, with a locally abundant sandy matrix. Vegetal remains are rare, and no fossils were encountered (De Santis et al., 2013).

5.1.2. Interpretation

Thick packages of gravels and sands with concave-up geometry, erosional base, fining-upward trends and lack of fossils reflect a high-energy, continental depositional environment and are interpreted as fluvial-channel deposits (Miall, 1992). The high ratio of bedload versus suspended load and poor sorting suggest braided stream facies that accumulated in steep gradient environments under strong morphological confinement.

5.2. Inner estuary

5.2.1. Description

This facies association, up to 13 m thick in core MAN (Fig. 4), is made up predominantly of bioturbated silt and clay. In its lower part (8 m in Fig. 4), it is varicolored, with abundant yellowish and reddish mottles due to Fe oxides (facies WdF in Fig. 5a), and locally hardened, with

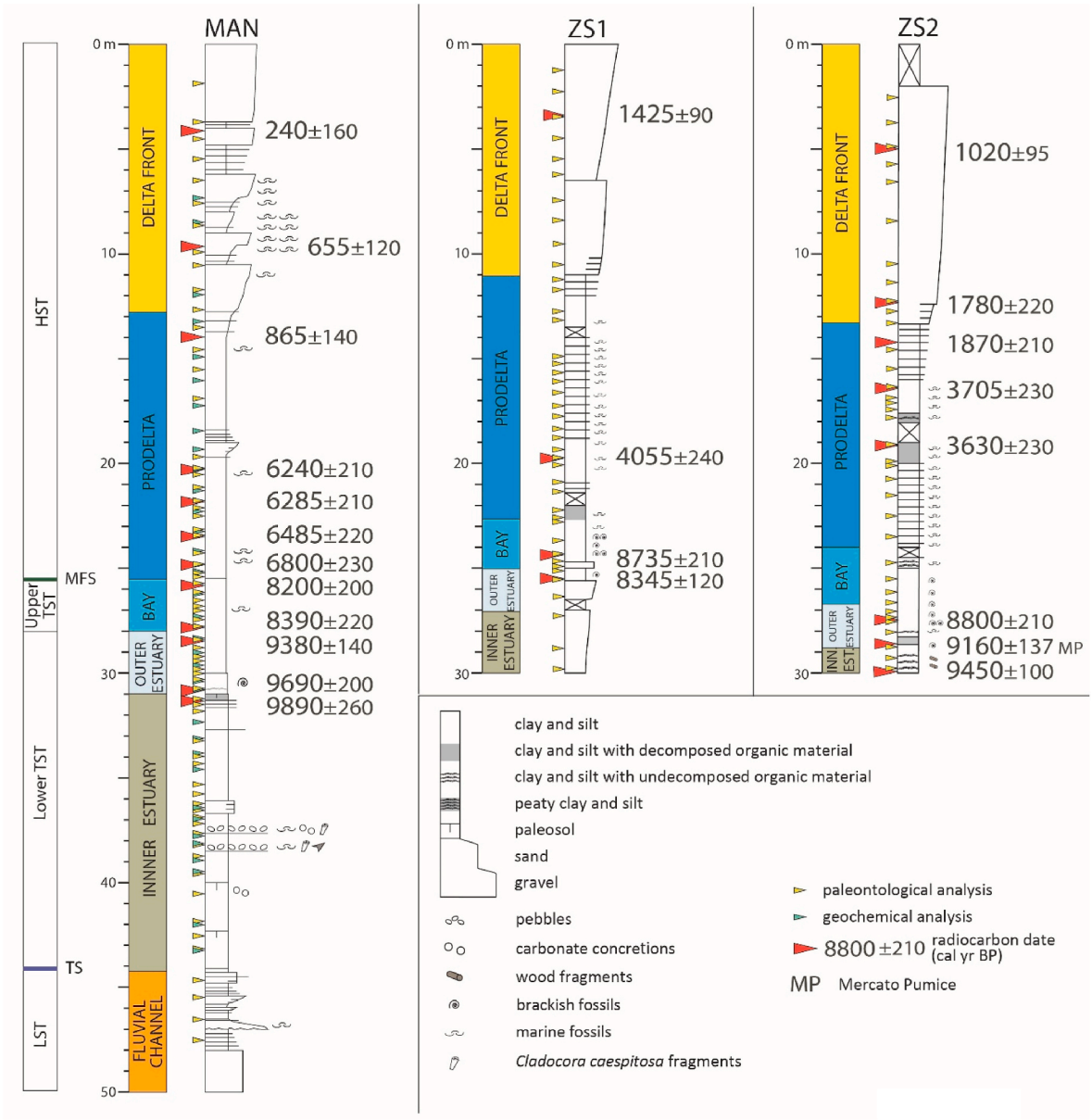

Fig. 4. Sedimentology and sequence-stratigraphic interpretation of reference cores MAN, ZS1, and ZS2 (see Fig. 1 for location), with stratigraphic position of samples for radiocarbon, paleontological and geochemical analyses.

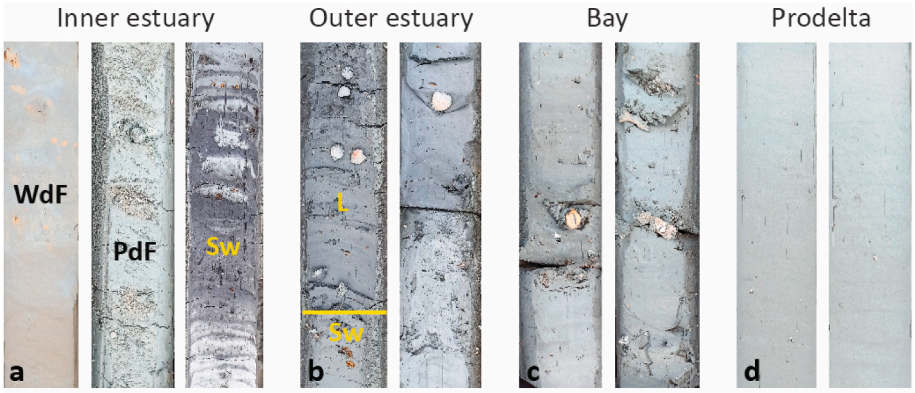

Fig. 5. Representative core photographs of the Manfredonia paleovalley fill (core bottom: lower left corner; core top: upper right corner). All photographs from core MAN (see Fig. 1 for location). a: 43-42 m core depth (WdF), 32-31 core depth (PdF and Sw); b: 31-30 m core depth; c: 28-27 m core depth; d: 18-17 m core depth. WdF: well-drained floodplain, PdF: poorly-drained floodplain, Sw: swamp, L: lagoon.

pocket penetration values invariably >2.5 kg/cm^2. Higher values, around 4–6 kg/cm^2, were observed in stiff clays with an abundance of mm-to cm-sized carbonate nodules. Upsection, this facies association exhibits a greenish grey color, root traces and occasional mottles due to Mn and Fe oxides (facies PdF in Fig. 5a). Silty sand and sand layers, generally less than 30 cm thick, are subordinate. Sharp-based sand bodies, up to 5 m thick, are locally embedded in the clay. Pocket-penetration tests record values in the range of 1.7–2.5 kg/cm^2. The uppermost part of this facies association, < 1 m thick in core MAN, consists of soft, organic-matter-rich clay, with a characteristic dark color, an abundance of plant debris, wood fragments and peat (facies Sw in Fig. 5a). Pocket penetration values in this stratigraphic interval drop to 0.4–0.9 kg/cm^2.

Macrofossils are rare. Coral fragments (*Cladocora caespitosa*), rare *Bittium* sp. and *Varicorbula gibba*, and rare specimens of the pulmonated gastropod *Cernuella* sp. were encountered around 37–38 m core depth (Fig. 4). Only rare and poorly preserved foraminifera, such as *Ammonia, Bulimina, Globigerina, Globigerinoides,* and *Gyroidina* were observed within this facies association. The uppermost layers show abundant hydrobiids, thin-shelled *Cerastoderma glaucum* and rare *Abra segmentum* plus few fragments of pulmonated gastropods. Specimens of freshwater ostracods (*Pseudocandona*) were locally recognized in cores ZS1 and ZS2.

5.2.2. Interpretation

The dominance of stiff, varicolored and oxidized fine-grained material grading upward to homogeneous silt and clay with lack of oxidation and generally low soil consistency suggest that deposition of this facies association took place in a fluvial-dominated, low-energy, well-drained (facies WdF) to poorly-drained (facies PdF) floodplain environment with low to high groundwater table, occasionally inundated by overflow waters. Isolated sand bodies likely reflect single-thread rivers (Potter et al., 1967; Hayes, 1975). The presence of indurated horizons and carbonate concretions is suggestive of local soil development. Based on its remarkable thickness and diagnostic fossil content (freshwater ostracods), this unit is argued to represent overbank sedimentation in a laterally confined environment, such as the inner part of an estuary, in which poorly preserved foraminifers and the rare mollusk fauna are interpreted to represent reworking of Pleistocene deposits (De Santis et al., 2010). Within facies Sw, dark grey to black colors reflect high proportion of organic matter. Abundant undecomposed vegetal remains, peat layers and very low (<1 kg/cm^2) pocket penetration values associated to common hydrobiids, rare brackish and thin-shelled bivalves reflect ephemeral bodies of stagnant waters under generally reducing conditions, such as hypohaline swamps adjacent to brackish marshes (Quarta et al., 2019).

5.3. Outer estuary facies association

This facies association, 2–3 m thick in reference cores (Fig. 4), is dominated by a homogeneous succession of soft clay and silty clay, with faint silt laminae, a few mm to cm thick. At the transition to underlying swamp clays, this unit exhibits dark grey color, plant debris and wood fragments (Fig. 5b). Upsection, the color is lighter grey. No pedogenic features were observed. Pocket penetration tests yielded values in the range of 0.7–1.0 kg/cm^2.

Within facies L (Fig. 5b), samples show a very similar stock of mollusk species represented by abundant, cm-sized shells (hydrobiids, *Cerastoderma glaucum*, and *Abra segmentum*). In the uppermost part of the unit, *Bittium reticulatum*, ostreids and rissoids are also abundant.

The meiofauna assemblage is dominated by well-preserved euryaline foraminifers and ostracods, such as *Ammonia tepida, Haynesina germanica* and *Cyprideis torosa*, with subordinate other foraminifers commonly found in lagoon settings (*Ammonia parkinsoniana, Aubignyna perlucida, Cribroelphidium gunteri, Elphidium fichtelianum, Elphidium oceanense, Porosononion granosum, Miliolinella* spp., and *Quinqueloculina seminulum*). Poorly preserved specimens of *Adelosina* and *Triloculina* are locally present.

5.3.1. Interpretation

This sedimentary unit is dominated by a low-diversity meiofauna able to tolerate changes in salinity and organic matter content. The macrobenthic associations recovered has been well documented in Quaternary paralic successions of Italy (e.g., Amorosi et al., 2014; Scarponi et al., 2017) and all over the Mediterranean (Pérès and Picard, 1964). As a whole, this facies association likely accumulated in a low-energy, mesohaline environment subject to short-lived salinity fluctuations, such as an outer estuary. The upward increase in mollusk taxa distributed also in shallow-marine settings (*Bittium*, ostreids, and rissoids) suggests development of less confined (more open) and higher-salinity conditions (Cau et al., 2019). Similarly, poorly preserved specimens of *Adelosina* and *Triloculina* are interpreted as transported from nearby marine environments.

5.4. Bay facies association

This facies association, about 2.5 m thick in reference cores (Fig. 4), consists of homogeneous medium grey clays with an abundance of body fossils concentrated at discrete horizons (Fig. 5c). A condensed fossil horizon was observed at 25.7 m depth in core MAN. From a lithological perspective, this unit is hardly distinguishable from underlying outer estuarine deposits, which have similar geotechnical characteristics (pocket penetration values between 0.8 and 1.0 kg/cm^2).

Within this facies association, the macrobenthic assemblage is characterized by a diversified stock of brackish species, with an upward increasing number of fully marine species, variable mollusk content and taphonomic damages. The lower part of this unit shows ecologically mixed assemblages of brackish to shallow-marine taxa (e.g., *Cerastoderma* and nuculids, respectively) with variable taphonomic damage (i.e., from pristine to highly damaged shells), mainly represented by bioerosion, chemical dissolution and encrustation. The topmost sample (at 25.7 m core depth) records an ecologically coherent stock of marine taxa represented by *Varicorbula gibba, Antalis* cf. *dentalis* (both common), and rare *Kurtiella bidentata, Sorgenfreispira brachystoma, Cerithidium submammilatum* and other mud-loving taxa. In core ZS2, the mollusk stock is mainly represented by *Ostea edulis*, *Modiolus barbatus*, and *Kurtiella bidentata*. Upwards, it is enriched in several marine taxa (e.g., *K. bidentata*, *Nucula nitidosa*, *Abra nitida*, and *Antalis inaequicostatum*).

The meiofauna is dominated by benthic foraminifera, mainly *Ammonia tepida, Aubignyna perlucida, Haynesina depressula, Elphidium* spp., *Porosononion granosum, Porosononion lidoense, Quinqueloculina seminulum* and several *Triloculina* species (*T. affinis, T. inflata* and *T. trigonula*). Other Milioloidea, such as *Adelosina, Miliolinella* and other *Quinqueloculina* are subordinate. Low amounts of *Ammonia beccarii, Ammonia parkinsoniana, Cribroelphidium* spp., and *Rosalina bradyi* are commonly observed.

5.4.1. Interpretation

Within this stratigraphic interval, mollusk assemblages record the rapid transition from oligotypic assemblages, typical of an open lagoon setting to a more open, marine habitat, such as a relatively sheltered embayment (Maselli et al., 2014), as suggested by the more diversified marine fauna and the abundance of ostreids in the upper part of this unit. The 50 cm-thick fossil-rich interval between 27.2 and 26.7 m, characterized by variable taphonomic damages and variable mollusk content, is retained to represent a transgressive lag. Finally, the relatively rich mollusk association retrieved at 25.8 m records a typical assemblage characterizing the transition to shelf marine environments commonly between 20 and 40 m water depth in the Adriatic Sea (e.g., Kowalewski et al., 2015; Scarponi et al., 2017; Tomašových et al., 2019).

The microfossil assemblage exhibits the particular co-occurrence of species tolerant (*Ammonia tepida, Aubignyna perlucida, Quinqueloculina seminulum and* Porosononion spp.*)* or sensitive (*Adelosina* spp., *Ammonia*

parkinsoniana, *Miliolinella* spp. and *Triloculina trigonula*) to organic matter enrichment (Jorissen et al., 2018). These species are considered to reflect a shallow-marine environment moderately influenced by river water. The presence of epiphytic taxa (*Triloculina trigonula* and *Rosalina bradyi*) indicates local vegetation cover at the sea bottom.

In general, the faunal assemblage displays the highest species diversity and relative abundance of open-marine species and thus reflects the deepest water depths attained during the Holocene.

5.5. Prodelta facies association

This facies association, up to 12 m thick, is dominated by homogenous light grey clay (Fig. 5d), with common silt intercalations. Sand layers are abundant in the upper part of this unit and show a characteristic upward increase in thickness and frequency. Plant debris and other organic matter are locally observed. Pocket penetration values are very low (0.5–0.7 kg/cm^2). The boundary with underlying bay deposits is transitional and has poor lithologic expression. It is, however, recognizable under visual inspection of the core by the sudden disappearance of large shells.

Within this 10-m-thick stratigraphic interval, all samples hold an ecologically compatible set of mollusk taxa, with abundant *Turritellinella tricarinata*, nuculids, *Kurtiella bydentata* and *Antalis* sp., and rare *Abra prismatica*, *Bela brachystoma* (among others) and *Varicorbula gibba*. In core ZS2, the most common species are *Moerella distorta*, *Varicorbula gibba*, *Kurtiella bidentata*, *Pitar rudis*, *Gouldia minima*, *A. nitida*, *Lembulus pella*, *Nucula nitidosa*, and *Antalis inaequicostatum*. Many ossicles of Asteroidea and vertebrae of Ophiuroidea are present.

The benthic foraminifera assemblage includes the same species found in the underlying bay facies association, but with remarkable differences in the relative abundance of individual taxa. In particular, an overall increase in *Ammonia tepida, Aubignyna perlucida, Porosononion granosum* and *Porosononion lidoense* is paralleled by the decrease in Milioloidea and *Elphidium* species.

5.5.1. Interpretation

The assemblage retrieved in this facies association is well documented from Pleistocene and Holocene muddy units of the Mediterranean basin (Angeletti and Scarponi, 2008; Scarponi et al., 2014, 2017; Rossi et al., 2021). This assemblage points toward marine muddy substrates characterized by moderate to sustained sedimentation rates. The relatively high diversity and turnover of the dominant mollusk species suggest episodic sedimentation.

As a whole, the faunal stock is commonly retrieved in marine environments typified by high rates of deposition. High amounts of foraminiferal taxa tolerant to organic matter enrichment (Jorissen et al., 2018) are typical of the prodelta and reveal a progressive increase in river influence (e.g., Barbieri et al., 2017). Occasional, thin-bedded intercalations of very-fine to fine sand, with sharp base and fining-upward trend, represent flood layers (Pellegrini et al., 2021), though the delta front (topset)–prodelta (foreset) transition is not resolved geometrically (Trincardi et al., 2020).

5.6. Prograding delta front/beach barrier

This facies association, up to 14 m thick, displays a gradational lower boundary to the prodelta/offshore facies association. It is made up predominantly of upward-coarsening and shallowing packages of well sorted, fine to medium sand separated by finer-grained intervals, 1–3 m thick, including silt admixed with very fine sand and abundant sand intercalations. This unit has a morphological expression, cropping out in elongate beach ridges parallel to the modern shoreline. On vertical profiles, silt-interlamination frequency and thickness decrease upwards.

In the lower part of this facies association, the mollusk content is relatively well diversified: the most abundant species are *Dosinia lupinus* and *Moerella distorta*, rare *V. gibba* and *Tritia* spp., along with a long list of other shallow-marine mollusks. Upwards, samples are represented by a well-diversified stock of species, mostly (semi-)infaunal or associated to seagrass cover and living in coastal environments with muddy-sands and sands (e.g., *Acanthocardia tuberculata*, *Loripes orbiculatus*, and various nassarids, tellinids and rare donacids species), together with epiphytic taxa (e.g., *B. reticulatum)* and species of wave-protected environments (*Lucinella divaricata*). This latter is abundant in nearly all samples. *Glycymeris nummaria* and *Donax* increase upwards. The upper 4 m show a relatively rich mollusk association, dominated by *Loripes orbiculatus, Donax semistriatus* and *D. trunculus*, along with a variety of rare epifaunal or byssally attached taxa that prefer hard or mixed substrates (e.g., *Arca noae*). The uppermost samples record rare pulmonated gastropods (*Cochlicella* spp.) or are barren, with only fragments of shallow-marine mollusks.

In the lower part of this facies association, the benthic foraminiferal assemblage includes high amounts of *Ammonia beccarii, A. tepida, Aubignyna perlucida, Porosononion granosum, P. lidoense* and Milioloidea (mainly *Adelosina* and *Triloculina*); *Rosalina bradyi* is locally common. Microfossils become progressively less abundant upwards, where *Ammonia beccarii* and Milioloidea are dominant, with common evidence of abrasion and size selection.

5.6.1. Interpretation

The mollusk fauna of this facies association is typical of shoreface Mediterranean settings (SFBC unit in Pérès and Picard, 1964) and the general abundance of sand reflects deposition above the storm wave base. Paucity of sand in the lower part of this facies association indicates a lower-energy depositional regime.

Ecological requirements of the retrieved mollusk species point toward coarser-grained settings (transition to lower shoreface environments). The presence of species living in wave-protected environments (*L. divaricata*) and ephiphyte taxa (e.g., *B. reticulatum*), however, suggests a more heterogeneous substrate with quieter areas (see also Crippa et al., 2019).

Upwards, the increase of donacis, and especially G. *nummaria*, which can also thrive in low-salinity settings (e.g., Crnčević et al., 2013), suggests river-influenced, upper delta front settings. The paucity of fossil remains, the presence of sub-fossilized shoreface diagnostic taxa and land snails suggest a coarse-grained or mixed, upper shoreface to foreshore environments transitioning upwards to backshore deposits. Indeed, the pulmonated retrieved are present in sandy and dry habitats, like vegetated dunes (Grano and Di Giuseppe, 2021).

The foraminiferal assemblage is consistent with a coastal environment with moderate fluvial influence and with a shallowing-upward trend, as documented by the number and preservation state of specimens observed in the upper part of the unit.

6. Geochemical signature of valley-fill deposits

According to previous work from the Southern Adriatic area (Cattaneo et al., 2003; Weltje and Brommer, 2011; Goudeau et al., 2013), the Gulf of Manfredonia and the adjacent Apulian offshore receive sediment from two major sources (Fig. 1): (i) direct supply from the Southern Apennines, with Candelaro, Cervaro, Carapelle and Ofanto river catchments as major feeding sources; (ii) significant, though subordinate, mixed sediment contribution from the Po River (Fig. 1) and Central Apennine rivers, via the Western Adriatic Current.

Sediment dispersal from the Central Apennines and the Po River delta occurs preferentially through SSE-directed transport pathways. A powerful longshore drift under dominant southerly currents has been ascertained by a large number of studies in the Western Adriatic area (Cattaneo et al., 2003; Ravaioli et al., 2003; Weltje and Brommer, 2011; Goudeau et al., 2013; Spagnoli et al., 2008, 2014, 2021; Rovere et al., 2019). The Po River is the main source of trace metals into the Western Adriatic Sea and accounts for 45–50% of Cr and Ni delivered to the mud wedge along the Western Adriatic shelf (Lopes-Rocha et al., 2017).

It has been documented that chromium is a trace element able to fingerprint local source-rock composition from mafic/ultramafic successions. This key marker can carry clear provenance signals even in distal segments of the routing system (von Eynatten et al., 2003; Amorosi, 2012; Garzanti, 2016; Sarti et al., 2020). As sediment composition also reflect hydraulic sorting (Garzanti et al., 2009), normalization of geochemical data using one element as grain size proxy is necessary to compensate for mineralogical and granular variability of metal concentrations.

A characteristic element ratio that has been tested successfully as a geochemical marker of sediment provenance from the Po River catchment is Cr/V (Amorosi and Sammartino, 2007). This ratio, which proved very effective in reducing the grain size effect, exhibits distinctly higher values for sediment generated from mafic/ultramafic (ophiolite) sources, irrespective of sample lithology. In particular, prodelta deposits collected at the Po River mouth yielded a mean Cr/V value of 1.69 (Amorosi et al., 2008).

In order to capture the geochemical signature of local (ophiolite-free) source rocks versus possibly Po-derived (ophiolite-bearing) sediment contribution, we applied the Cr/V ratio to 16 inner-estuary (freshwater) and 17 outer-estuary (brackish) to marine deposits from core MAN, and matched these values against 11 samples from Apulian rivers (Candelaro, Cervaro, Carapelle and Ofanto), which we used as a Southern Apennine end-member (Fig. 6; Supplementary Table 2).

Vertical changes in trace metal contents within transgressive, valley-fill deposits are interpreted to reflect changes in the relative contribution of fluvial (ophiolite-free) versus marine (ophiolite-bearing) supply (Fig. 6): in particular, the mean Cr/V value of inner-estuarine samples (0.84) is slightly higher than the mean value of Apulian river deposits (0.82), whereas the maximum Cr/V value (0.88) is recorded up-section, within outer-estuarine to open-marine samples.

Although the prominence of the Gargano Promontory may represent an obstacle to SE-directed currents along the Western Adriatic mud belt, systematically increasing Cr/V values from hinterland (alluvial) to inner-estuarine and outer-estuarine/marine environments are interpreted to reflect mixed contribution from transversal (southern Apennines) and longitudinal (Po River + central Apennines) sediment sources, thus supporting the hypothesis of conspicuous alongshore sediment transport from the Po River to the Apulian offshore via the Western Adriatic Current.

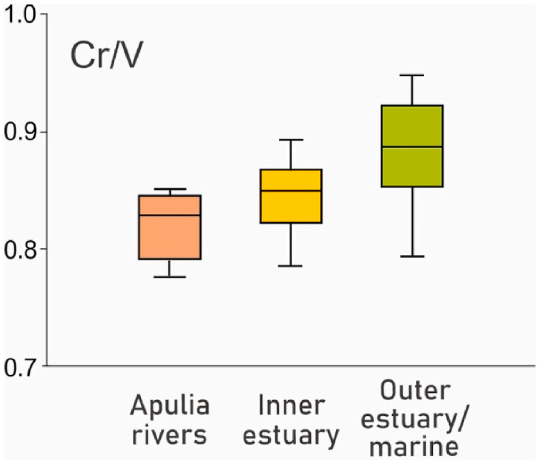

Fig. 6. Box plots of Cr/V ratios for fluvial, inner estuary, and outer estuary/marine muds from core MAN, showing increasing values with increasing marine influence. The lower boundary of each box is the 25th percentile, the upper boundary is the 75th percentile, the bold line within the box corresponds to the median, the "whiskers" define the minimum and maximum values.

7. Stratigraphic architecture of apulian paleovalleys

The internal anatomy of three Apulian paleovalleys, linked to the Candelaro, Cervaro and Carapelle rivers, respectively, was reconstructed through a 17-km-long stratigraphic panel oriented roughly parallel to the modern shoreline and transversal to the paleovalley axes (Fig. 7). Along the transect, all paleovalley systems show prominent paleotopography (25–30 m relief), with width/thickness ratios around 150–200 (narrow sheets of Gibling, 2006). The Candelaro paleovalley represents the inland sector of the Manfredonia incised valley identified in shelf areas by Maselli and Trincardi (2013), Maselli et al. (2014) and De Santis and Caldara (2016). The Cervaro and Carapelle paleovalleys are the updip counterparts of the paleovalleys identified in offshore position by De Santis et al. (2020a, b – Fig. 3).

In general, there is close correspondence between the vertical stacking of fluvial, inner-estuarine, outer-estuarine, bay, prodelta and delta front deposits reconstructed from core analysis (Fig. 7) and seismostratigraphic stacking patterns of paleovalley systems identified offshore (Fig. 3). Integrated sedimentological and paleontological analysis of sediment cores allows to define the key surfaces for sequence-stratigraphic interpretation (Zecchin et al., 2021).

The sequence boundary (SB) at the base of paleovalley systems is a prominent stratigraphic surface that is clearly recognizable from seismic profiles (Fig. 3). This erosional surface truncates much older marine strata attributable to the MIS5e coastal prism (De Santis et al., 2010; Maselli et al., 2014), indicating deep fluvial incision along major drainage axes. The basal valley-fill surface is marked (i) by the base of laterally amalgamated fluvial-channel gravel or sand bodies, up to 5 km wide, or (ii) by the sharp contrast between soft (valley-fill) deposits and stiff continental deposits into which valleys are incised (Fig. 7). Though poor quality stratigraphic descriptions provide no clear evidence of soil formation at the valley margin, we used overconsolidation as an indicator of the interfluve sequence boundary (Amorosi et al., 2017b). Highly dissected, narrow interfluve surfaces with thin, lenticular gravel bodies, interpreted as fluvial terraces, suggest periods of floodplain degradation that we interpreted as forced regressive deposits or Bond-scale falling-stage systems tract (Csato et al., 2014 - FSST in Fig. 7).

The complete sedimentary succession records three distinct stages in the evolution of the valley fill (Fig. 7), represented by seismic units 1–3 (Fig. 3). Sharp-based, amalgamated gravel or sand bodies in the lower parts of paleovalley fills (seismic unit 1) testify to a period of persistent channel activity likely attributable to lowstand conditions (lowstand systems tract or LST) and that may accord with a LGM attribution (Maselli and Trincardi, 2013), although these strata are not chronologically constrained by dates.

The abrupt boundary between sheet-like, amalgamated fluvial bodies and overlying lenticular bodies isolated within a mud-dominated, well-drained floodplain succession (facies WdF) marks the change from low-accommodation to relatively higher-accommodation conditions, which is traditionally interpreted as the landward expression of the initial transgressive surface (Shanley and McCabe, 1991, 1994; Labourdette and Jones, 2007; Catuneanu, 2017). Changes in the geometry of fluvial-channel bodies and their association with abundant floodplain deposits reflect development into the valley of a muddy floodplain with narrow and deep, single-thread alluvial streams (Aslan and Autin, 1999; Kasse et al., 2010; Li et al., 2010; Tanabe, 2020), which is interpreted to reflect the fluvial-estuarine transition.

The abundance of poorly-drained floodplain deposits (facies PdF) indicates that early stages of transgression in the study area were accompanied by fluvial aggradation in a strongly confined environment (Maselli and Trincardi, 2013 - seismic unit 2), landward of the transgressive estuarine-marine limit (lower transgressive systems tract or TST). Although this portion of the valley fill is not constrained chronologically, we tentatively assign this unit to the Lateglacial. The thin, dark interval rich in wood debris penetrated by the study cores atop the lower estuarine unit (facies Sw) yielded dates ranging between about 9.9 and

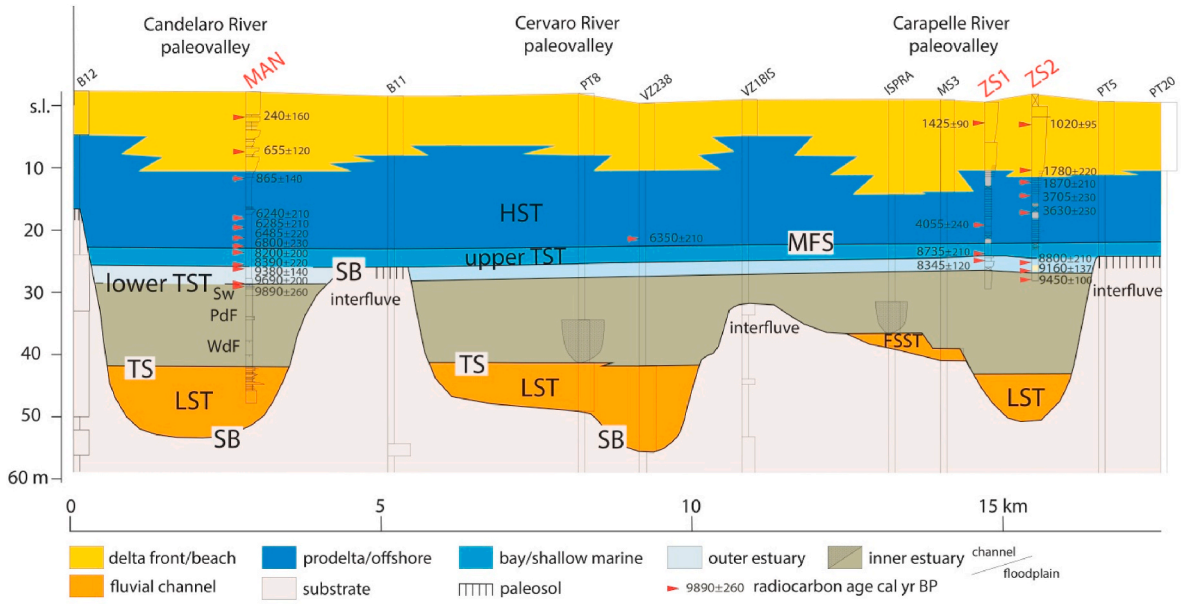

Fig. 7. Stratigraphic architecture of Candelaro, Cervaro and Carapelle paleovalleys. Compare with seismic line interpretations in Figs. 2 and 3. FSST: falling-stage systems tract, LST: lowstand systems tract, TST: transgressive systems tract, HST: highstand systems tract, SB: sequence boundary, TS: transgressive surface, MFS: maximum flooding surface. WdF: well-drained floodplain, PdF: poorly-drained floodplain, Sw: swamp.

9.5 cal kyr B.P. (Fig. 7). This unit records transgressive inundation of a coastal setting, with rapid transition to generalized wetland sub-environments.

The vertical succession of inner estuary to outer estuary deposits observed in cores MAN, ZS1 and ZS2 is mostly associated with incised valley systems that were typically filled as sea-level rise promoted accommodation increase during transgression (Dalrymple et al., 1994; Zaitlin et al., 1994). Between about 9.5 and 9.2 cal kyr B.P., the three paleovalley fills record a deepening-upward trend that reflects transgressive influx of brackish waters. Outer-estuarine deposits are laterally confined (seismic unit 3 in Fig. 3) and there is no indication of early transgressive deposition above the valley margins, which were still undergoing degradation (and likely pedogenesis) during valley filling.

The stratigraphic surface that demarcates the estuarine-marine transition is dated to about 8.5 cal kyr B.P. and is interpreted to represent the boundary between the lower and upper TST (Figs. 4 and 7). Although this surface has poor lithologic expression, being represented by a clay-on-clay contact, the boundary between brackish (estuarine) clay and overlying bay/open marine clay has a diagnostic fossil signature, bearing invariably strong indication of increasing salinity and relative deepening. This surface can be correlated above three distinct paleovalley fills (Fig. 7) and has regional stratigraphic significance.

The development of an open-marine environment testifies to the filling of the valleys, with subsequent basinwide flooding of the interfluves. This prominent paleoenvironmental change is marked by the boundary between laterally confined estuarine deposits and poorly confined to unconfined bay deposits (Fig. 7). At the valley margins, where no lowstand or early transgressive deposition occurred, upper TST deposits directly overlie the interfluve sequence boundary (McCarthy and Plint, 1998) and SB merges with the transgressive surface. Higher up in the stratigraphic column, discrete shell layers within the bay/open-marine succession are interpreted to represent fossil lags due transgressive reworking, probably associated with renewed eustatic rise during the Early Holocene.

A surface of stratigraphic condensation is recorded atop the bay/open-marine facies association: this condensed interval, chronologically constrained between 8.0 and 7.0 cal kyr B.P. (Fig. 7), includes the maximum flooding surface (MFS). The MFS has a combined taphonomic evidence: (i) the mixing of autochthonous taxa, forming a concentration of relatively well-diversified skeletal parts, and (ii) the presence of highly damaged shells and encrusting biota (Scarponi et al., 2017). At this stratigraphic level, the mollusk content is dominated by *V. gibba*, *K. bidentata* along with scaphopods (i.e., *Antalis*). The abundance of *K. bidentata* also points out to the presence of ophiuroid-dominated communities (Ockelmann and Muss, 1978). Based on present-day environmental requirements (Oliver et al., 2016) and estimated preferential bathymetric distribution of the retrieved mollusk taxa (Wittmer et al., 2014), a depositional environment bracketed between 10 m and 30 m water depth can be hypothesized.

A normal regressive stacking pattern typifies the highstand systems tract (HST), where superposed prodelta and delta front facies associations indicate enhanced sediment flux under relatively stable sea-level conditions.

The response of transgressive units to stepped, post-LGM sea-level rise has been widely documented on Central Mediterranean shelves (Zecchin et al., 2015). In the southern Adriatic, it has been recently reconstructed offshore Apulia, within the Ofanto incised valley (Fig. 1), where short-lived progradation of coastal barrier complexes was interrupted by rapid relative sea-level rise linked to increased rate of ice melting and eustatic rise, namely meltwater pulses 1A and 1B (De Santis et al., 2020a).

In this study, through identification of two flooding surfaces, formed around 9.5 and 8.0 cal kyr B.P., respectively, and across which there is evidence of a relative increase in water depth (onset of brackish conditions and maximum marine ingression, respectively), we reconstructed two additional phases of rapid relative sea-level rise that have clear expression on land. Coeval backstepping of estuarine environments locally associated with stratigraphic condensation has been recorded in other paleovalley systems of the Adriatic area (Amorosi et al., 2016, 2017a; Ronchi et al., 2021; Campo et al., 2022) and worldwide (Hori et al., 2004; Sloss et al., 2005; Hijma et al., 2009; Zong et al., 2009; Simms et al., 2010; Tanabe et al., 2015). Based on radiocarbon dating, the two flooding surfaces identified in the Manfredonia paleovalley system coincide with meltwater pulses 1C and 1D, at 9.5–9.0 and 8.0–7.0 cal kyr B.P., respectively (Blanchon et al., 2002; Liu et al., 2004), suggesting that abrupt deepening was driven primarily by sea level.

8. Conclusions

We reconstructed a Late Pleistocene to Holocene history of valley excavation and infill in the Southern Adriatic region through combined sedimentological, paleoecological and geochemical analysis of three sediment cores from onshore Apulia and their comparison with offshore seismic stratigraphy. Sequence stratigraphic interpretation, chronologically constrained by 25 radiocarbon dates, provides an integrated picture of multiple valley and interfluve development in which stratigraphic architecture of paleovalley fills was largely driven by relative sea-level changes.

Above coarse-grained fluvial deposits that form the amalgamated lower paleovalley fill, the upper valley fill includes a vertical succession of mud-dominated, inner to outer estuary deposits. These, in turn, are overlain by bay/open-marine clays and by a shallowing-upward succession of prodelta and delta front facies associations. Stratigraphic discontinuities characterize the valley interfluves, where Holocene transgressive deposits overlie indurated and pedogenized, pre-LGM deposits. Three stratigraphically significant surfaces were recognized: the sequence boundary and the transgressive surface have clear sedimentologic expression, whereas the maximum flooding surface demarcates subtle changes in paleoecological features and is marked by a condensed section.

Geochemical fingerprinting of inner-estuary deposits reveals enhanced sediment supply from Apulian river catchments in the early stages of paleovalley filling. Increasing contribution of material sourced from mafic/ultramafic rocks at the fluvial-marine transition is interpreted to reflect influence of the SE-directed (longshore) Western Adriatic current, which carries the unique (Cr-rich) compositional signature of Po River sediments.

This study shows that integrated paleoecological data, including mollusks, benthic foraminifers and ostracods are highly effective in assisting the paleoenvironmental interpretation of late Quaternary paleovalley successions. The dramatic paleoenvironmental change linked to Holocene valley filling and basinwide interfluve flooding corresponds on seismic profiles to the obvious transition from laterally confined to unconfined settings. In the core record, though lacking a clear lithologic expression, this stratigraphic surface is readily identified by its diagnostic paleoecological signature.

Declaration of competing interest

The authors declare that they have no known competing financial interests or personal relationships that could have appeared to influence the work reported in this paper.

Data availability

Data will be made available on request.

Acknowledgments

This work was supported by the Italian Ministry of University and Research under the PRIN 2017 program, project number 2017ASZAKJ "*The Po-Adriatic Source-to-Sink system (PASS): from modern sedimentary processes to millennial-scale stratigraphic architecture*", grant to Alessandro Amorosi. The funding source had no involvement in study design; in the collection, analysis and interpretation of data; in the writing of the report; and in the decision to submit the article for publication. We thank Claudio Di Celma and an anonymous reviewer for their constructive criticism.

Appendix A. Supplementary data

Supplementary data to this article can be found online at https://doi.org/10.1016/j.marpetgeo.2022.105975.

References

Abdulah, K.C., Anderson, J.B., Snow, J.N., Holdford-Jack, L., 2004. The Late Quaternary Brazos and Colorado deltas, offshore Texas, USA—their evolution and the factors that controlled their deposition. In: Anderson, J.B., Fillon, R.H. (Eds.), Late Quaternary Stratigraphic Evolution of the Northern Gulf of Mexico Margin, vol. 79. SEPM Special Publication, pp. 237–269.

Amorosi, A., 2012. Chromium and nickel as indicators of source-to-sink sediment transfer in a Holocene alluvial and coastal system (Po Plain, Italy). Actual. Models Sediment Gener. 280, 260–269. https://doi.org/10.1016/j.sedgeo.2012.04.011.

Amorosi, A., Sammartino, I., 2007. Influence of sediment provenance on background values of potentially toxic metals from near-surface sediments of Po coastal plain (Italy). Int. J. Earth Sci. 96, 389–396. https://doi.org/10.1007/s00531-006-0104-8.

Amorosi, A., Dinelli, E., Rossi, V., Vaiani, S.C., Sacchetto, M., 2008. Late Quaternary palaeoenvironmental evolution of the Adriatic coastal plain and the onset of Po River Delta. Palaeogeogr. Palaeoclimatol. Palaeoecol. 268, 80–90. https://doi.org/10.1016/j.palaeo.2008.07.009.

Amorosi, A., Rossi, V., Sarti, G., Mattei, R., 2013. Coalescent valley fills from the late Quaternary record of Tuscany (Italy). Quat. Int. 288, 129–138.

Amorosi, A., Rossi, V., Scarponi, D., Vaiani, S.C., Ghosh, A., 2014. Biosedimentary record of postglacial coastal dynamics: high-resolution sequence stratigraphy from the northern Tuscan coast (Italy). Boreas 43, 939–954. https://doi.org/10.1111/bor.12077.

Amorosi, A., Bracone, V., Campo, B., D'Amico, C., Rossi, V., Rosskopf, C.M., 2016. A late Quaternary multiple paleovalley system from the Adriatic coastal plain (Biferno River, Southern Italy). Geomorphology 254, 146–159.

Amorosi, A., Bruno, L., Campo, B., Morelli, A., Rossi, V., Scarponi, D., Hong, W., Bohacs, K.M., Drexler, T.M., 2017a. Global sea-level control on local parasequence architecture from the Holocene record of the Po Plain. Italy. Mar. Petrol. Geol. 87, 99–111.

Amorosi, A., Bruno, L., Cleveland, D.M., Morelli, A., Hong, W., 2017b. Paleosols and associated channel-belt sand bodies from a continuously subsiding late Quaternary system (Po Basin, Italy): new insights into continental sequence stratigraphy. Geol. Soc. Am. Bull. 129, 449–463. https://doi.org/10.1130/B31575.1.

Anderson, J.B., Rodriguez, A., Abdulah, K.C., Fillon, R.H., Banfield, L.A., McKeown, H.A., Wellner, J.S., 2004. Late quaternary stratigraphic evolution of the northern Gulf of Mexico margin: a synthesis. In: Anderson, J.B., Fillon, R.H. (Eds.), Late Quaternary Stratigraphic Evolution of the Northern Gulf of Mexico Margin, vol. 79. SEPM Special Publication, pp. 1–23. https://doi.org/10.2110/pec.04.79.0001.

Aslan, A., Autin, W.J., 1999. Evolution of the Holocene Mississippi River floodplain, Ferriday, Louisiana; insights on the origin of fine-grained floodplains. J. Sediment. Res. 69, 800–815. https://doi.org/10.2110/jsr.69.800.

Athersuch, J., Horne, D.J., Whittaker, J.E., 1989. Marine and brackish water ostracods (superfamilies Cypridacea and Cytheracea): Keys and notes for the identification of the species. In: New Series) 43. Brill E.J., Leiden.

Autin, W.J., Aslan, A., 2001. Alluvial pedogenesis in Pleistocene and Holocene Mississippi River deposits: effects of relative sea-level change. Geol. Soc. Am. Bull. 113, 1456–1466.

Barbieri, G., Amorosi, A., Vaiani, S.C., 2017. Benthic foraminifera as a key to delta evolution: a case study from the late Holocene succession of the Po River Delta. Micropaleontology 63, 27–41.

Blanchon, P., Jones, B., Ford, D.C., 2002. Discovery of a submerged relic reef and shoreline off Grand Cayman: further support for an early Holocene jump in sea level. Sediment. Geol. 147, 253–270.

Blum, M.D., Price, D.M., 1998. Quaternary alluvial plain construction in response to glacio-eustatic and climatic controls, Texas Gulf coastal plain. In: Shanley, K.W., McCabe, P.J. (Eds.), Relative Role of Eustacy, Climate, and Tectonism in Continental Rocks, vol. 59. SEPM Special Publication, pp. 31–48.

Blum, M.D., Törnqvist, T.E., 2000. Fluvial responses to climate and sea-level change: a review and look forward. Sedimentology 47, 2–48.

Blum, M., Martin, J., Milliken, K., Garvin, M., 2013. Paleovalley systems: insights from Quaternary analogs and experiments. Earth Sci. Rev. 116, 128–169.

Boenzi, F., Caldara, M., Pennetta, L., 1991. Stratigraphic and geomorphological observations in the southern part of the Tavoliere coastal plain. Apulia. Geogr. Fis. e Din. Quat. 14, 23–31.

Boyd, R., Dalrymple, R., Zaitlin, B., 2006. Estuarine and incised-valley facies models. In: Posamentier, H.W., Walker, R.G. (Eds.), Facies Models Revisited, vol. 84. SEPM Special Publication, pp. 171–235.

Bronk Ramsey, C., 2009. Bayesian analysis of radiocarbon dates. Radiocarbon 51, 337–360. https://doi.org/10.1017/S0033822200033865.

Busschers, F.S., Kasse, C., Van Balen, R.T., Vandenberghe, J., Cohen, K.M., Weerts, H.J.T., Wallinga, J., Johns, C., Cleveringa, P., Bunnik, F.P.M., 2007. Late Pleistocene evolution of the Rhine-Meuse system in the southern North Sea basin: imprints of climate change, sea-level oscillation and glacio-isostacy. Quat. Sci. Rev. 26, 3216–3248.

Caldara, M., Pennetta, L., 1991. Pleistocenic buried abrasion platforms in southeastern "Tavoliere" (Apulia, south Italy). Alp. Mediterr. Quat. 4, 303–309.

Caldara, M., Pennetta, L., 1993. Nuovi dati per la conoscenza geologica e morfologica del Tavoliere di Puglia. Bonifica 8, 25–42.

Cattaneo, A., Correggiari, A., Langone, L., Trincardi, F., 2003. The late-Holocene Gargano subaqueous delta, Adriatic shelf: sediment pathways and supply fluctuations. Mar. Geol. 193, 61–91. https://doi.org/10.1016/S0025-3227(02)00614-X.

Catuneanu, O., 2017. Chapter one - sequence stratigraphy: guidelines for a standard methodology. In: Montenari, M. (Ed.), Stratigraphy & Timescales. Academic Press, pp. 1–57. https://doi.org/10.1016/bs.sats.2017.07.003.

Cau, S., Laini, A., Monegatti, P., Roveri, M., Scarponi, D., Taviani, M., 2019. Palaeocological anatomy of shallow-water Plio-Pleistocene biocalcarenites (northern Apennines, Italy). Palaeogeogr. Palaeoclimatol. Palaeoecol. 514, 838–851. https://doi.org/10.1016/j.palaeo.2018.08.011.

Ciaranfi, N., Loiacono, F., Moretti, M., 2011. Note illustrative della Carta Geologica d'Italia alla scala 1: 50.000. In: Foglio 408 'Foggia.' Litografia Artist. Cartogr. Firenze.

Cimerman, F., Langer, M., 1991. Mediterranean foraminifera: Slovenska akademija znanosti in umetnosti. Acad. Sci. Artium Slov. Ljubl. 30, 118.

Crippa, G., Azzarone, M., Bottini, C., Crespi, S., Felletti, F., Marini, M., Petrizzo, M.R., Scarponi, D., Raffi, S., Raineri, G., 2019. Bio- and lithostratigraphy of lower Pleistocene marine successions in western Emilia (Italy) and their implications for the first occurrence of Arctica islandica in the Mediterranean Sea. Quat. Res. 92, 549–569. https://doi.org/10.1017/qua.2019.20.

Crnčević, M., Peharda, M., Ezgeta-Balić, D., Pećarević, M., 2013. Reproductive cycle of glycymeris nummaria (Mollusca: Bivalvia) from Mali Ston bay, Adriatic Sea, Croatia. Sci. Mar. 77, 293–300.

Csato, I., Catuneanu, O., Granjeon, D., 2014. Millennial-scale sequence stratigraphy: numerical simulation with dionisos. J. Sediment. Res. 84, 394–406.

Dabrio, C.J., Zazo, C., Goy, J.L., Sierro, F.J., Borja, F., Lario, J., Gonzalez, J.A., Flores, J. A., 2000. Depositional history of estuarine infill during the last postglacial transgression (Gulf of Cadiz, Southern Spain). Mar. Geol. 162, 381–404.

Dalrymple, R.W., 2006. Incised valleys in time and space: an introduction to the volume and an examination of the controls on valley formation and filling. In: Dalrymple, R. W., Leckie, D.A., Tillman, R.W. (Eds.), Incised Valleys in Time and Space, vol. 85. SEPM Special Publication, pp. 5–12.

Dalrymple, R.W., Boyd, R., Zaitlin, B.A., 1994. Incised-Valley Systems: Origin and Sedimentary Sequences, vol. 51. SEPM Special Publication, pp. 1–391.

De Santis, V., Caldara, M., 2016. Evolution of an incised valley system in the southern Adriatic Sea (Apulian margin): an onshore–offshore correlation. Geol. J. 51, 263–284.

De Santis, V., Caldara, M., de Torres, T., Ortiz, J.E., 2010. Stratigraphic units of the Apulian Tavoliere plain (Southern Italy): chronology, correlation with marine isotope stages and implications regarding vertical movements. Sediment. Geol. 228, 255–270. https://doi.org/10.1016/j.sedgeo.2010.05.001.

De Santis, V., Caldara, M., Pennetta, L., 2013. The marine and alluvial terraces of Tavoliere di Puglia plain (southern Italy). J. Maps 10, 114–125. https://doi.org/10.1080/17445647.2013.861366.

De Santis, V., Caldara, M., Torres, T., Ortiz, J.E., 2014. Two middle Pleistocene warm stages in the terrace deposits of the Apulia region (southern Italy). Quat. Int. 332, 2–18. https://doi.org/10.1016/j.quaint.2013.10.009.

De Santis, V., Caldara, M., Pennetta, L., 2020a. Continuous" backstepping of Holocene coastal barrier systems into incised valleys: insights from the Ofanto and Carapelle-Cervaro valleys. Water 12, 1799.

De Santis, V., Caldara, M., Pennetta, L., 2020b. Transgressive architecture of coastal barrier systems in the Ofanto incised valley and its surrounding shelf in response to stepped sea-level rise. Geosciences 10.12, 497. https://doi.org/10.3390/geosciences10120497.

De Santis, V., Caldara, M., Torres, T., Ortiz, J.E., Sánchez-Palencia, Y., 2020c. The role of beach ridges, spits, or barriers in understanding marine terraces processes on loose or semiconsolidated substrates: insights from the givoni of the Gulf of Taranto (southern Italy). Geol. J. 55 (4), 2951–2975. https://doi.org/10.1002/gj.3550.

De Stigter, H.C., Jorissen, F.J., van der Zwaan, G.J., 1998. Bathymetric distribution and microhabitat partitioning of live (Rose Bengal stained) benthic Foraminifera along a shelf to bathyal transect in the southern Adriatic Sea. J. Foraminifer. Res. 28, 40–65.

Debenay, J.-P., Guillou, J.-J., Redois, F., Geslin, E., 2000. Distribution trends of foraminiferal assemblages in paralic environments. In: Martin, R.E. (Ed.), Environmental Micropaleontology: the Application of Microfossils to Environmental Geology, Topics in Geobiology. Springer US, Boston, MA, pp. 39–67. https://doi.org/10.1007/978-1-4615-4167-7_3.

Doglioni, C., 1991. A proposal for the kinematic modelling of W-dipping subductions - possible applications to the Tyrrhenian-Apennines system. Terra. Nova 3, 423–434. https://doi.org/10.1111/j.1365-3121.1991.tb00172.x.

Doglioni, C., Mongelli, F., Pieri, P., 1994. The Puglia uplift (SE Italy): an anomaly in the foreland of the Apenninic subduction due to buckling of a thick continental lithosphere. Tectonics 13, 1309–1321. https://doi.org/10.1029/94TC01501.

Doglioni, C., Harabaglia, P., Martinelli, G., Mongelli, F., Zito, G., 1996. A geodynamic model of the Southern Apennines accretionary prism. Terra. Nova 8, 540–547. https://doi.org/10.1111/j.1365-3121.1996.tb00783.x.

Ellis, B.F., Messina, A.R., 1940. Catalogue of Foraminifera. The American Museum of Natural History, New York.

Ellis, B.F., Messina, A.R., 1952. Catalogue of Ostracoda. The American Museum of Natural History, New York.

Fan, D., Shang, S., Burr, G., 2019. Sea level implications from late quaternary/holocene paleosols from the Oujiang Delta, China. Radiocarbon 61, 83–99.

Frezza, V., Carboni, M.G., 2009. Distribution of recent foraminiferal assemblages near the Ombrone River mouth (northern Tyrrhenian sea, Italy). Rev. Micropaleontol. 52, 43–66. https://doi.org/10.1016/j.revmic.2007.08.007.

Garzanti, E., 2016. From static to dynamic provenance analysis—sedimentary petrology upgraded. Sediment. Geol. 336, 3–13. https://doi.org/10.1016/j.sedgeo.2015.07.010.

Garzanti, E., Andò, S., Vezzoli, G., 2009. Grain-size dependence of sediment composition and environmental bias in provenance studies. Earth Planet Sci. Lett. 277, 422–432. https://doi.org/10.1016/j.epsl.2008.11.007.

Gibling, M.R., 2006. Width and thickness of fluvial channel bodies and valley fills in the geological record: a literature compilation and classification. J. Sediment. Res. 76, 731–770.

Gibling, M.R., Fielding, C.R., Sinha, R., 2011. Alluvial valleys and alluvial sequences. Towards a geomorphic assessment. In: Davidson, S.K., Leleu, S., North, C. (Eds.), From River to Rock Record: the Preservation of Fluvial Sediments and Their Subsequent Interpretation, vol. 97. SEPM Special Publication, pp. 423–447.

Goudeau, M.-L.S., Grauel, A.-L., Bernasconi, S.M., de Lange, G.J., 2013. Provenance of surface sediments along the southeastern Adriatic coast off Italy: an overview. Estuar. Coast Shelf Sci. 134, 45–56. https://doi.org/10.1016/j.ecss.2013.09.009.

Grano, M., Giuseppe, R.D., 2021. I molluschi terrestri e dulciacquicoli (Mollusca: gastropoda, Bivalvia) di Castel di Guido (Lazio, Italia centrale) Checklist preliminare. Boll. Mus. Reg. Sci. Nat. Torino 38, 149–168.

Hayes, M.O., 1975. Morphology of sand accumulation in estuaries: an introduction to the symposium. In: Cronin, L.E. (Ed.), Geology and Engineering. Academic Press. Academic Press, pp. 3–22. https://doi.org/10.1016/B978-0-12-197502-9.50006-X.

Henderson, P.A., 1990. Freshwater Ostracods: Keys and Notes for the Identification of the Species, New Series 42. Linnean Society of London and the Estuarine and Coastal Sciences Association, Leiden.

Hijma, M.P., Cohen, K.M., Hoffmann, G., Van der Spek, A.J.F., Stouthamer, E., 2009. From river valley to estuary: the evolution of the Rhine river mouth in the early to middle Holocene (western Netherlands, Rhine-Meuse delta). Neth. J. Geosci. 88, 13–53.

Hori, K., Tanabe, S., Saito, Y., Haruyama, S., Nguyen, V., Kitamura, A., 2004. Delta initiation and holocene sea-level change: example from the Song Hong (red river) delta, Vietnam. Sediment. Geol. 164, 237–249.

Jorissen, F.J., 1988. Benthic foraminifera from the Adriatic Sea : principles of phenotypic variation. Utrecht Micropaleontol. Bull. 37, 176.

Jorissen, F., Nardelli, M.P., Almogi-Labin, A., Barras, C., Bergamin, L., Bicchi, E., El Kateb, A., Ferraro, L., McGann, M., Morigi, C., Romano, E., Sabbatini, A., Schweizer, M., Spezzaferri, S., 2018. Developing Foram-AMBI for biomonitoring in the Mediterranean: species assignments to ecological categories. Mar. Micropaleontol. 140, 33–45. https://doi.org/10.1016/j.marmicro.2017.12.006.

Kasse, C., Bohncke, S.J.P., Vandenberghe, J., Gábris, G., 2010. Fluvial style changes during the last glacial–interglacial transition in the middle Tisza valley (Hungary). Fluv. Rec. Arch. Hum. Act. Environ. Change 121, 180–194. https://doi.org/10.1016/j.pgeola.2010.02.005.

Kowalewski, M., Wittmer, J.M., Dexter, T.A., Amorosi, A., Scarponi, D., 2015. Differential responses of marine communities to natural and anthropogenic changes. Proc. R. Soc. B Biol. Sci. 282, 20142990 https://doi.org/10.1098/rspb.2014.2990.

Labaune, C., Tesson, M., Gensous, B., Parize, O., Imbert, P., Delhaye-Prat, V., 2010. Detailed architecture of a compound incised valley system and correlation with forced regressive wedges: example of Late Quaternary Têt and Agly rivers, western Gulf of Lions, Mediterranean Sea. France. Sediment. Geol. 223, 360–379.

Labourdette, R., Jones, R.R., 2007. Characterization of fluvial architectural elements using a three-dimensional outcrop data set: escanilla braided system, South-Central Pyrenees, Spain. Geosphere 3, 422–434. https://doi.org/10.1130/GES00087.1.

Li, C., Chen, Q., Zhang, J., Yang, S., Fan, D., 2000. Stratigraphy and paleoenvironmental changes in the Yangtze delta during the late quaternary. J. Asian Earth Sci. 18, 453–469.

Li, W., Bhattacharya, J.P., Campbell, C., 2010. Temporal evolution of fluvial style in a compound incised-valley fill, Ferron "Notom delta". Henry Mountains Region, Utah (U.S.A.). J. Sed. Res. 80, 529–549.

Liu, J.P., Milliman, J.D., Gao, S., Cheng, P., 2004. Holocene development of the Yellow River's subaqueous delta, north Yellow Sea. Mar. Geol. 209, 45–67.

Lopes-Rocha, M., Langone, L., Miserocchi, S., Giordano, P., Guerra, R., 2017. Spatial patterns and temporal trends of trace metal mass budgets in the western Adriatic sediments (Mediterranean Sea). Sci. Total Environ. 1022–1033. https://doi.org/10.1016/j.scitotenv.2017.04.114, 599–600.

Malinverno, A., Ryan, W.B.F., 1986. Extension in the Tyrrhenian Sea and shortening in the Apennines as result of arc migration driven by sinking of the lithosphere. Tectonics 5, 227–245. https://doi.org/10.1029/TC005i002p00227.

Maselli, V., Trincardi, F., 2013. Large-scale single incised valley from a small catchment basin on the western Adriatic margin (central Mediterranean Sea). Global Planet. Change 100, 245–262.

Maselli, V., Trincardi, F., Asioli, A., Ceregato, A., Rizzetto, F., Taviani, M., 2014. Delta growth and river valleys: the influence of climate and sea level changes on the South Adriatic shelf (Mediterranean Sea). Quat. Sci. Rev. 99, 146–163.

Mattheus, C.R., Ramsey, K.W., Tomlinson, J.L., 2020. The evolution of coastal-plain incised valleys over multiple glacio-eustatic cycles: insights from the inner continental shelf of Delaware, USA. J. Sediment. Res. 90, 1510–1526. https://doi.org/10.2110/jsr.2020.69.

Mazzini, I., Marrone, F., Arculeo, M., Rossetti, G., 2017. Revision of recent and fossil *Mixtacandona* Klie 1938 (Ostracoda, Candonidae) from Italy, with description of a new species. Zootaxa 4221. https://doi.org/10.11646/zootaxa.4221.3.3 zootaxa.4221.3.3.

Mazzini, I., Aiello, G., Frenzel, P., Pint, A., 2022. Marine and marginal marine Ostracoda as proxies in geoarchaeology. Mar. Micropaleontol. 174, 102054 https://doi.org/10.1016/j.marmicro.2021.102054.

McCarthy, P.J., Plint, G.A., 1998. Recognition of interfluve sequence boundaries: integrating paleopedology and sequence stratigraphy. Geology 26, 387–390. https://doi.org/10.1130/0091-7613(1998)026<0387:ROISBI>2.3.CO;2.

Miall, A.D., 1992. Facies models, response to sea level change. Geol. Assoc. Can. 119–142.

Milker, Y., Schmiedl, G., 2012. A taxonomic guide to modern benthic shelf foraminifera of the western Mediterranean Sea. Palaeontol. Electron. 15 (2), 134p. https://doi.org/10.26879/271, 16A.

Mitchum Jr., R.M., Vail, P.R., Sangree, J.B., 1977. Seismic stratigraphy and global changes of sea level, Part 6: stratigraphic interpretation of seismic reflection patterns in depositional sequences. Section 2. Application of seismic reflection configuration to stratigraphic interpretation. In: Payton, C.E. (Ed.), Seismic Stratigraphy — Applications to Hydrocarbon Exploration, vol. 26. Am. Ass. Petrol. Geol. Memoir, pp. 117–133. https://doi.org/10.1306/M26490C8.

Murray, J.W., 2006. Ecology and Applications of Benthic Foraminifera. Cambridge University Press, Cambridge.

Ockelmann, K.W., Muss, K., 1978. The biology, ecology and behaviour of the bivalve *Mysella bidentata* (Montagu). Ophelia 17, 1–93.

Oliver, P.G., Holmes, A.M., Killeen, I.J., Turner, J. A.m, 2016. Marine bivalve shells of the British Isles. Amgueddfa Cymru - National Museum Wales. Available from: http://naturalhistory.museumwales.ac.uk/britishbivalves.

Patacca, E., Scandone, P., 1989. Post-Tortonian mountain building in the Apennines. The role of the passive sinking of a relic lithospheric slab. Accad. Naz. Dei Lincei, Atti dei Convegni Lincei 80, 157–176.

Patacca, E., Scandone, P., 2001. Late thrust propagation and sedimentary response in the thrust-belt—foredeep system of the Southern Apennines (Pliocene-Pleistocene). In: Vai, G.B., Martini, I.P. (Eds.), Anatomy of an Orogen: the Apennines and Adjacent Mediterranean Basins. Springer Netherlands, Dordrecht, pp. 401–440. https://doi.org/10.1007/978-94-015-9829-3_23.

Pellegrini, C., Maselli, V., Cattaneo, A., Piva, A., Ceregato, A., Trincardi, F., 2015. Anatomy of a compound delta from the post-glacial transgressive record in the Adriatic Sea. Mar. Geol. 362, 43–59. https://doi.org/10.1016/j.margeo.2015.01.010.

Pellegrini, C., Patruno, S., Helland-Hansen, W., Steel, R.J., Trincardi, F., 2020. Clinoforms and clinothems: Fundamental elements of basin infill. Basin Res. 32, 187–205. https://doi.org/10.1111/bre.12446.

Pellegrini, C., Tesi, T., Schieber, J., Bohacs, K.M., Rovere, M., Asioli, A., Nogarotto, A., Trincardi, F., 2021. Fate of terrigenous organic carbon in muddy clinothems on continental shelves revealed by stratal geometries: insight from the Adriatic sedimentary archive. Global Planet. Change 203, 103539. https://doi.org/10.1016/j.gloplacha.2021.103539.

Pérès, J.M., Picard, J., 1964. Nouveau manuel de bionomie benthique. Recueil des Travaux de la Station marine d'Endoume 31.47, 1–137.

Posamentier, H.W., Vail, P.R., 1988. Eustatic controls on clastic deposition II—sequence and systems tract models. In: Wilgus, C.K., Hastings, B.S., Kendall, C.G.StC., Posamentier, H.W., Ross, C.A., Van Wagoner, J.C. (Eds.), Sea-Level Changes: an Integrated Approach, vol. 42. SEPM Special Publication, pp. 125–154. https://doi.org/10.2110/pec.88.01.0125.

Posamentier, H.W., Jervey, M.T., Vail, P.R., 1988. Eustatic controls on clastic deposition I—conceptual framework. In: Wilgus, C.K., Hastings, B.S., Kendall, C.G.StC., Posamentier, H.W., Ross, C.A., Van Wagoner, J.C. (Eds.), Sea-Level Changes: an Integrated Approach, vol. 42. SEPM Special Publication, pp. 109–124. https://doi.org/10.2110/pec.88.01.0109.

Potter, P.E., 1967. Sand bodies and sedimentary environments: a review. Am. Assoc. Petrol. Geol. Bull. 51, 337–365.

Quarta, G., Fago, P., Calcagnile, L., Cipriano, G., D'Elia, M., Moretti, M., Scardino, G., Valenzano, E., Mastronuzzi, G., 2019. 14C age offset in the mar Piccolo sea basin in Taranto (southern Italy) estimated on Cerastoderma glaucum (Poiret, 1789). Radiocarbon 61, 1387–1401. https://doi.org/10.1017/RDC.2019.38.

Ravaioli, M., Alvisi, F., Vitturi, L.M., 2003. Dolomite as a tracer for sediment transport and deposition on the northwestern Adriatic continental shelf (Adriatic Sea, Italy). Continent. Shelf Res. 23, 1359–1377. https://doi.org/10.1016/S0278-4343(03)00121-3.

Reimer, P.J., Austin, W.E.N., Bard, E., Bayliss, A., Blackwell, P.G., Bronk Ramsey, C., Butzin, M., Cheng, H., Edwards, R.L., Friedrich, M., Grootes, P.M., Guilderson, T.P., Hajdas, I., Heaton, T.J., Hogg, A.G., Hughen, K.A., Kromer, B., Manning, S.W., Muscheler, R., Palmer, J.G., Pearson, C., Van Der Plicht, J., Reimer, R.W., Richards, D.A., Scott, E.M., Southon, J.R., Turney, C.S.M., Wacker, L., Adolphi, F., Büntgen, U., Capano, M., Fahrni, S.M., Fogtmann-Schulz, A., Friedrich, R., Köhler, P., Kudsk, S., Miyake, F., Olsen, J., Reinig, F., Sakamoto, M., Sookdeo, A., Talamo, S., 2020. The IntCal20 northern Hemisphere radiocarbon age calibration curve (0-55 cal kBP). Radiocarbon 62, 725–757. https://doi.org/10.1017/RDC.2020.41.

Ricchetti, G., Ciaranfi, N., Luperto Sinni, E., Mongelli, F., Pieri, P., 1992. Geodinamica ed evoluzione sedimentaria e tettonica dell'avampaese apulo. Mem. Soc. Geol. Ital. 41, 57–82.

Rittenour, T.M., Goble, R.J., Blum, M.D., 2005. Development of an OSL chronology for Late Pleistocene channel belts in the lower Mississippi valley, USA. Quat. Sci. Rev. 24, 2539–2554.

Ronchi, L., Fontana, A., Cohen, K.M., Stouthamer, E., 2021. Late Quaternary landscape evolution of the buried incised valley of Concordia Sagittaria (Tagliamento River, NE Italy): a reconstruction of incision and transgression. Geomorphology 373, 107509. https://doi.org/10.1016/j.geomorph.2020.107509.

Rossi, V., Vaiani, S.C., 2008. Benthic foraminiferal evidence of sediment supply changes and fluvial drainage reorganization in Holocene deposits of the Po Delta. Italy. Mar. Micropaleontol. 69, 106–118. https://doi.org/10.1016/j.marmicro.2008.07.001.

Rossi, V., Barbieri, G., Vaiani, S.C., Amorosi, A., 2021. Benthic foraminifers from Holocene subaqueous deltas of the Western Mediterranean: stratigraphic implications and palaeoenvironmental significance of the biofacies. Mar. Geol. 442, 106632 https://doi.org/10.1016/j.margeo.2021.106632.

Rovere, M., Pellegrini, C., Chiggiato, J., Campiani, E., Trincardi, F., 2019. Impact of dense bottom water on a continental shelf: an example from the SW Adriatic margin. Mar. Geol. 408, 123–143. https://doi.org/10.1016/j.margeo.2018.12.002.

Royden, L., Patacca, E., Scandone, P., 1987. Segmentation and configuration of subducted lithosphere in Italy: an important control on thrust-belt and foredeep-basin evolution. Geology 15, 714–717. https://doi.org/10.1130/0091-7613(1987)15<714:SACOSL>2.0.CO;2.

Salel, T., Bruneton, H., Lefèvre, D., 2016. Ostracods and environmental variability in lagoons and deltas along the north-western Mediterranean coast (Gulf of Lions, France and Ebro delta, Spain). Rev. Micropaleontol. 59, 425–444. https://doi.org/10.1016/j.revmic.2016.09.001.

Sangree, J.B., Widmier, J.M., 1977. Seismic stratigraphy and global changes of sea level, part 9: seismic interpretation of clastic depositional facies. Section 2. Application of seismic reflection configuration to stratigraphic interpretation. In: Payton, C.E. (Ed.), Seismic Stratigraphy — Applications to Hydrocarbon Exploration, vol. 26. Am. Ass. Petrol. Geol. Memoir, pp. 165–184. https://doi.org/10.1306/M26490C11.

Sarti, G., Sammartino, I., Amorosi, A., 2020. Geochemical anomalies of potentially hazardous elements reflect catchment geology: an example from the Tyrrhenian coast of Italy. Sci. Total Environ. 714, 136870 https://doi.org/10.1016/j.scitotenv.2020.136870.

Scarponi, D., Kowalewski, M., 2004. Stratigraphic paleoecology: bathymetric signatures and sequence overprint of mollusk associations from upper Quaternary sequences of the Po Plain. Italy. Geology 32, 989–992. https://doi.org/10.1130/G20808.1.

Scarponi, D., Angeletti, L., 2008. Integration of palaeontological patterns in the sequence stratigraphy paradigm: a case study from Holocene deposits of the Po Plain (Italy). Geoacta 7, 1–13.

Scarponi, D., Huntley, J.W., Capraro, L., Raffi, S., 2014. Stratigraphic paleoecology of the Valle di Manche section (Crotone basin, Italy): a candidate GSSP of the middle Pleistocene. Palaeogeogr. Palaeoclimatol. Palaeoecol. 402, 30–43. https://doi.org/10.1016/j.palaeo.2014.02.032.

Scarponi, D., Azzarone, M., Kusnerik, K., Amorosi, A., Bohacs, K.M., Drexler, T.M., Kowalewski, M., 2017. Systematic vertical and lateral changes in quality and time resolution of the macrofossil record: insights from Holocene transgressive deposits, Po coastal plain. Italy. Mar. Petrol. Geol. 87, 128–136. https://doi.org/10.1016/j.marpetgeo.2017.03.031.

Scarponi, D., Nawrot, R., Azzarone, M., Pellegrini, C., Gamberi, F., Trincardi, F., Kowalewski, M., 2022. Resilient biotic response to long-term climate change in the Adriatic Sea. Global Change Biol. 28, 4041–4053. https://doi.org/10.1111/gcb.16168.

Sgarrella, F., Moncharmont Zei, M., 1993. Benthic foraminifera of the Gulf of Naples (Italy): systematics and autoecology. Boll. Soc. Paleontol. Ital. 32, 145–264.

Shanley, K.W., McCabe, P.J., 1991. Predicting facies architecture through sequence stratigraphy—an example from the Kaiparowits Plateau. Utah Geol. 19, 742–745. https://doi.org/10.1130/0091-7613(1991)019<0742:PFATSS>2.3.CO;2.

Shanley, K.W., McCabe, P.J., 1994. Perspectives on the sequence stratigraphy of continental Strata1. Am. Assoc. Petrol. Geol. Bull. 78, 544–568. https://doi.org/10.1306/BDFF9258-1718-11D7-8645000102C1865D.

Simms, A.R., Aryal, N., Miller, L., Yokoyama, Y., 2010. The incised valley of Baffin Bay, Texas: a tale of two climates. Sedimentology 57, 642–669.

Sloss, C.R., Jones, B.J., Murray-Wallace, C.V., McClennen, C.E., 2005. Holocene sea level fluctuations and the sedimentary evolution of a barrier estuary: lake Illawarra, new south Wales, Australia. J. Coastal Res. 215, 943–959.

Spagnoli, F., Bartholini, G., Dinelli, E., Giordano, P., 2008. Geochemistry and particle size of surface sediments of Gulf of Manfredonia (Southern Adriatic sea). Estuar. Coast Shelf Sci. 80, 21–30. https://doi.org/10.1016/j.ecss.2008.07.008.

Spagnoli, F., Dinelli, E., Giordano, P., Marcaccio, M., Zaffagnini, F., Frascari, F., 2014. Sedimentological, biogeochemical and mineralogical facies of northern and central western Adriatic Sea. J. Mar. Syst. 139, 183–203. https://doi.org/10.1016/j.jmarsys.2014.05.021.

Spagnoli, F., De Marco, R., Dinelli, E., Frapiccini, E., Frontalini, F., Giordano, P., 2021. Sources and metal pollution of sediments from a coastal area of the central western Adriatic Sea (southern Marche region, Italy). Appl. Sci. 11 https://doi.org/10.3390/app11031118.

Tanabe, S., 2020. Stepwise accelerations in the rate of sea-level rise in the area north of Tokyo Bay during the Early Holocene. Quat. Sci. Rev. 248, 106575.

Tanabe, S., Nakanishi, T., Ishihara, Y., Nakashima, R., 2015. Millennial-scale stratigraphy of a tide-dominated incised valley during the last 14 kyr: spatial and quantitative reconstruction in the Tokyo Lowland, central Japan. Sedimentology 62, 1837–1872.

Thomas, M.A., Anderson, J.B., 1994. Sea-level controls on the facies architecture of the Trinity/Sabine incised-valley system, Texas continental shelf. In: Dalrymple, R.W., Boyd, R., Zaitlin, B.A. (Eds.), Incised-Valley Systems: Origin and Sedimentary Sequences, vol. 51. SEPM Special Publication, pp. 63–82. https://doi.org/10.2110/pec.94.12.0063.

Tomašových, A., Gallmetzer, I., Haselmair, A., Kaufman, D.S., Mavrič, B., Zuschin, M., 2019. A decline in molluscan carbonate production driven by the loss of vegetated habitats encoded in the Holocene sedimentary record of the Gulf of Trieste. Sedimentology 66, 781–807. https://doi.org/10.1111/sed.12516.

Trincardi, F., Amorosi, A., Bosman, A., Correggiari, A., Madricardo, F., Pellegrini, C., 2020. Ephemeral rollover points and clinothem evolution in the modern Po Delta based on repeated bathymetric surveys. Basin Res. 32, 402–418.

Van Wagoner, J.C., Mitchum, R.M., Campion, K.M., Rahmanian, V.D., 1990. Siliciclastic sequence stratigraphy in well logs, cores, and outcrops: concepts for high-resolution correlation of time and facies. Am. Ass. Petrol. Geol. Methods Explor. 7, 3–55.

von Eynatten, H., Barceló-Vidal, C., Pawlowsky-Glahn, V., 2003. Composition and discrimination of sandstones: a statistical evaluation of different analytical methods. J. Sediment. Res. 73, 47–57. https://doi.org/10.1306/070102730047.

Wang, R., Colombera, L., Mountney, N.P., 2020. Quantitative analysis of the stratigraphic architecture of incised-valley fills: a global comparison of Quaternary systems. Earth Sci. Rev. 200, 102988.

Weltje, G.J., Brommer, M.B., 2011. Sediment-budget modelling of multi-sourced basin fills: application to recent deposits of the western Adriatic mud wedge (Italy). Basin Res. 23, 291–308.

Wittmer, J.M., Dexter, T.A., Scarponi, D., Amorosi, A., Kowalewski, M., 2014. Quantitative bathymetric models for late quaternary transgressive-regressive cycles of the Po plain. Italy. J. Geol. 122, 649–670. https://doi.org/10.1086/677901.

Wright, V.P., Marriott, S.B., 1993. The sequence stratigraphy of fluvial depositional systems: the role of floodplain sediment storage. Sediment. Geol. 86, 203–210.

Zaitlin, B.A., Dalrymple, R.W., Boyd, R., 1994. The stratigraphic organization of incised-valley systems associated with relative sea-level change. In: Dalrymple, R.W., Boyd, R., Zaitlin, B.A. (Eds.), Incised-Valley Systems: Origin and Sedimentary Sequences, vol. 51. SEPM Special Publication, pp. 45–60. https://doi.org/10.2110/pec.94.12.0045.

Zecchin, M., Ceramicola, S., Lodolo, E., Casalbore, D., Chiocci, F.L., 2015. Episodic, rapid sea-level rises on the central Mediterranean shelves after the Last Glacial Maximum: a review. Mar. Geol. 369, 212–223.

Zecchin, M., Caffau, M., Catuneanu, O., 2021. Recognizing maximum flooding surfaces in shallow-water deposits: an integrated sedimentological and micropaleontological approach (Crotone Basin, southern Italy). Mar. Petrol. Geol. 133, 105225.

Zong, Y., Yim, W.S., Yu, F., Huang, G., 2009. Late Quaternary environmental changes in the Pearl River mouth region, China. Quat. Int. 206, 35–45.